Robotic Intracardiac Catheter Steering System

MQP Report

A Major Qualifying Project By:

Megan DeSanty, Isabelle Lachaux, Elizabeth Minor, Rebecca Young

Advised By:

Haichong Zhang, Shang Gao, Loris Fichera, Zhenglun Alan Wei, Yihao Zheng

April 25th, 2024

Abstract

Over a million people in the U.S. undergo cardiac catheterization procedures every year [34]. The Siemens AcuNav ICE catheter uses ultrasound to image the heart internally, providing visual feedback for diagnosis and surgeries. The traditional method of performing a cardiac catheterization involves 2-6 hours of focused, exhausting work from the clinician [6]. Robotic control and actuation of the control knobs and pull wires would relieve the clinician of the tedious parts of the catheterization procedure [10]. This would produce more consistent results, reducing experience and fatigue-based variability [10]. This project aimed to reduce clinician involvement in navigating an ultrasound intracardiac catheter by developing a teleoperative robotic steering system. In the final prototype of this device, stepper motors power gears that rotate the catheter knobs and the entire handle of the catheter, providing three degrees of freedom. An Arduino Uno sends commands to the motor drivers based on keyboard inputs, allowing clinicians teleoperative control of the ICE catheter. The device is able to smoothly control the motion of the catheter tip and predict where the tip will be using a MATLAB simulation. This system builds the foundation for reducing clinician fatigue and eliminating variability in cardiac catheterization procedures.

List of Contents

List of Figures

Authorship Table

Section	Primary Author(s)	Secondary Author(s)
Abstract	Rebecca	
List of Contents	All	
List of Figures	All	
1. Background	All	
1.1 Client Statement	Rebecca	
1.2 Anatomy	Rebecca	
1.2.1 Heart & Functions	Rebecca	
1.2.2 Imaging	Rebecca	Isabelle
1.2.3 Catheter Procedures	Rebecca, Isabelle	
1.3 Mechanical	Isabelle	
1.3.1 Kinematics	Isabelle	
1.4 Robotic	Ellie, Megan	
1.4.1 Algorithms	Megan	
1.4.2 Proportional-Integral-Derivative (PID) Controller	Ellie	
1.4.2.1 Step Counts	Megan	
1.4.2.2 External Camera	Megan	
1.4.2.3 Serial Port Communication	Megan	
1.4.2.4 External Camera	Ellie	
1.4.3 Mapping Systems	Megan	
1.4.4 Chart of Specifications	Megan	
2. Methods and Implementation	All	
2.1 Iteration 1	All	

2.1.1 Mechanical	Isabelle	Rebecca
2.1.2 Hardware	Ellie	Megan
2.1.3 Software	Megan	Ellie
2.2 Iteration 2	All	
2.2.1 Mechanical	Rebecca, Isabelle	
2.2.2 Hardware	Ellie	Megan
2.2.3 Software	Megan	
2.3 Iteration 3	All	
2.3.1 Mechanical	Rebecca, Isabelle	
2.3.2 Hardware	Ellie, Megan	
2.3.3 Software	Ellie, Megan	
2.4 Final Design	Rebecca, Ellie	Isabelle
3. Results	Ellie	
4. Discussion	Rebecca, Megan	
5. Broader Impact	Rebecca	
5.1 Societal Impacts	Rebecca	
5.2 Environmental Impacts	Rebecca	
5.3 Economical Impacts	Rebecca	
5.4 Standards and Regulations	Rebecca	
6. References	All	

1. Background

1.1 Client Statement

The goal of this project is to develop a teleoperated robotic intracardiac catheter steering system to reduce the involvement of a clinician in the navigation of a catheter through the veins to the heart. Cardiac catheterization procedures are common across the U.S. with over a million people in the U.S. undergoing procedures each year. These procedures are a minimally invasive way to diagnose and treat issues in the heart, preferred to open heart surgery due to reduced length and strain on patients [5]. The average catheter procedure involves 2-6 hours of precise and exhausting work for the clinician in charge [6]. Developing a teleoperated catheter navigation system would alleviate the strain on the clinician, allowing them to focus on the more difficult and important parts of the procedure, such as device deployment. Rather than being fatigued from guiding a catheter through the network of veins towards the heart, reducing their active surgery time would result in a fresh, sharp mind going into difficult heart repairs. Development of this device could produce more consistent results, eliminating experience and fatigue-based variabilities [10]. New clinicians would not have to go through years of training to master routine tasks that can be completed by a robotic system [10]. As the technology and algorithms become more advanced, autonomous navigation has the potential to improve the accuracy of catheter manipulation and determine the optimal route through the vascular system. Integrating robotic steering eliminates the delay between the ultrasound probe and the clinician operating the catheter, allowing swift reactions to changing patient conditions within the veins [10].

1.2 Anatomy

1.2.1 Heart + Functions

The cardiovascular system is the body's extensive transportation network, consisting of the heart and blood vessels which pump nutrient and oxygen-rich blood to tissues across the body [14]. The heart is a muscle about the size of a fist which beats seventy to eighty times per minute to pump five liters of blood through the blood vessels [14]. Within the walls of the heart, three layers are present: the myocardium, consisting of cardiac muscle; the endocardium, an inner lining that reduces friction with the blood; and the pericardium, a thick sac that anchors the heart in the thoracic cavity [14].

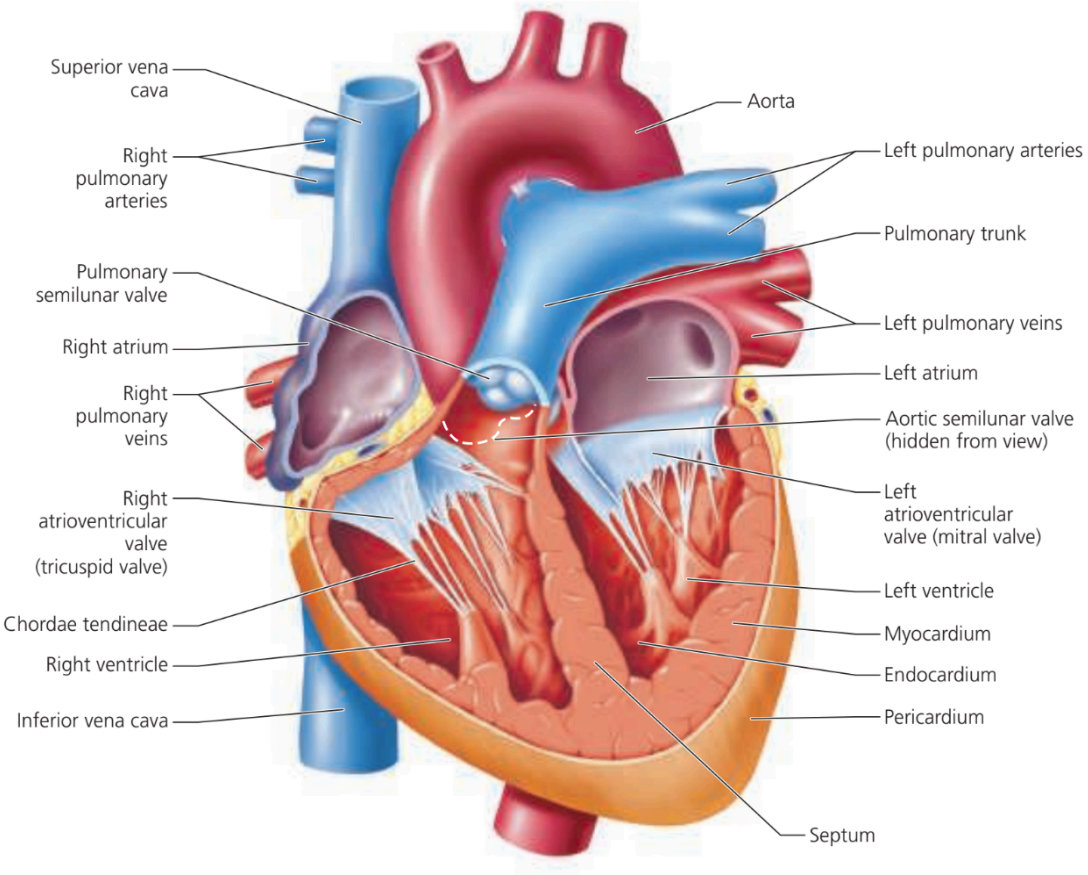

Figure 1: Ventral view of the human heart cut on the coronal plane to reveal the internal structures [14].

The structure of the heart is visible in Figure 1 above, displaying the two halves of the heart divided by the septum, with an atrium and ventricle in each [14]. The atria are the receiving chambers for blood returning to the heart, while the ventricles act as the main pumps forcing blood out of the heart [14]. Between these chambers, the atrioventricular valves are attached to the heart walls by connective tissue called chordae tendineae to prevent backflow of blood into the atria [14]. The right side of the heart contains a tricuspid valve with three flaps, while the left side has the mitral valve with two flaps [14]. Additionally, the semilunar valves sit between the ventricles and arteries to prevent backflow of blood into the ventricles when the pressure in the arteries is higher [14]. Once the blood leaves the heart, it is pumped through two circuits, the pulmonary circuit, on the right side of the heart, and the systemic circuit, on the left side [14]. In the pulmonary circuit, the blood is pumped from the right ventricle, through the pulmonary arteries to the lungs to obtain oxygen, and through the pulmonary veins back to the left atrium [14]. In the systemic circuit, the blood goes through the left atrium, is pumped from the left ventricle through the aorta to the capillary beds in body tissues [14]. It is then collected by the veins and transported through the superior and inferior vena cavas back to the right atrium [14].

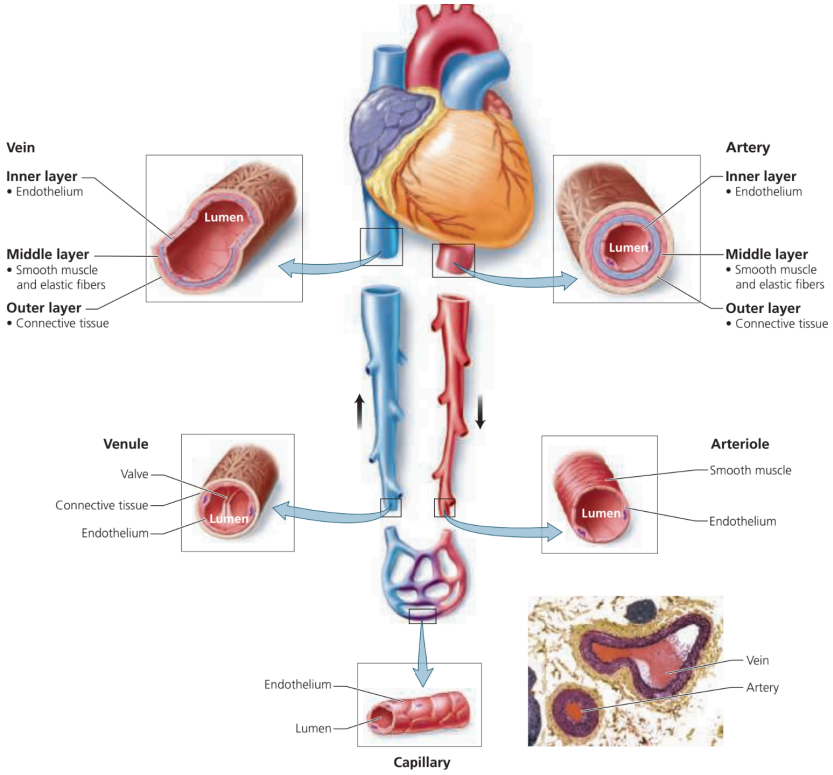

Figure 2: Breakdown of types of blood vessels [14].

The structure of the vessels that carry blood through the body must be considered during catheter development, as the way the catheter interacts with the body is important [14]. The basic structures of arteries, veins, venules, arterioles and capillaries are shown in Figure 2 above. Arteries and veins have a common structure, including three layers: the inner layer, the endothelium; a middle layer of elastic fibers and circular smooth muscle; and an outer layer of connective tissue [14]. Each layer has a function: the inner layer reduces friction with the blood, the middle layer allows the artery to contract and return to its original shape, and the outer layer adds strength to the wall and anchors the artery to the surrounding tissue [14]. Capillaries, on the other hand, have a slightly different structure, since they are specialized for exchange of materials [14]. The walls are only one cell layer thick and are clumped into capillary beds with 10-100 capillaries in each network [14]. Arterioles coming from the heart lead into capillaries and then the capillaries merge to form venules that bring blood back towards the heart [14]. These blood vessels branch out across the human body and form intricate networks to nourish body tissues and excrete waste products from cells [14].

1.2.2 Imaging

In order to visualize these networks, different types of imaging can be used which can help to guide a catheter through the body. Fluoroscopy involves the insertion of a contrast dye and x-rays passing through the body to allow clear visualization of veins throughout the procedure [16]. It is typically used in intravenous catheter insertion, however it entails risks due

to heavy radiation exposure to both the clinician and patient, and potential allergic reactions to the dye [16]. Another common imaging technique is ultrasound which would allow for continuous, real-time imaging of the cardiac anatomy [10]. This is a less harmful procedure using sound waves to produce images of cardiac structures and vessels [10]. Ultrasound is commonly used during device deployment, however the resulting images are noisy and have limited resolution [10]. One way of reducing the noise is to conduct the ultrasound from within the body, using a method such as transesophageal echocardiograms (TEE) [17]. In TEE, a probe with a transducer is inserted into the esophagus to reduce the disruption of sound waves by other tissues, ribs and heart [17]. This can be very helpful for getting a clear image of the heart structures while operating a catheter.

1.2.3 Catheter Procedures

Cardiac catheterization is a procedure where wires and sensors bound by a tube called a catheter are inserted into blood vessels in the patient's groin, arm, or neck and fed to the heart [34]. This procedure is a minimally invasive way for physicians to access a patient's heart to address various cardiac related issues as mentioned in the previous section. Along with the catheter device ultrasound and x-ray are commonly used to visualize and navigate the complex vascular systems of a patient.

Intravascular ultrasound catheters (IVUS) are primarily used presently for cardiac procedures. These catheters consist of a distal tip, distal shaft, proximal shaft and handle as shown in the diagram below [19]. The distal catheter tip is made of a hard material to guide the flexible wires through veins. The distal shaft is made of a soft and flexible material to allow for movement across several planes of motion. The proximal shaft is a hollow tube made of a material with high stiffness that also encases the pull wires. The pull wires are connected to the base of the distal tip to manipulate the bend of the distal shaft.

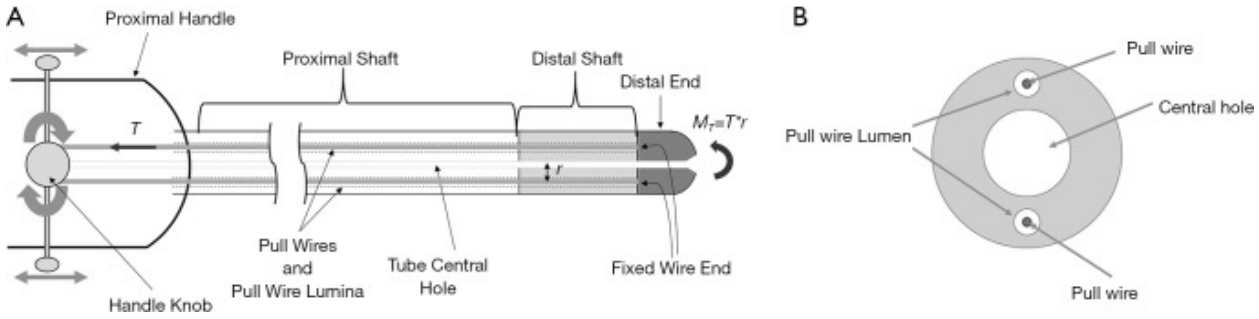

Figure 3: Diagram of a catheter's components along with a cross section of the proximal and distal shaft [19].

Below, Table 1 displays a list of cardiac conditions that intracardiac catheters could be used to diagnose. Cardiac catheterization is used to confirm these issues and to determine the severity.

Table 1: Cardiac conditions that can be assessed using the Siemens ICE catheter [7, 26].

Cardiac Condition	Description
Coronary Artery Disease	Plaque builds up in the arteries supplying blood to the heart, narrowing the arteries and reducing blood flow [7].
Valvular Diseases	Issues with any of the four heart valves (aortic, mitral, pulmonary, and tricuspid) can result in decreased heart function [12]. There are three main types of valvular diseases - atresia, where the valve has no opening, preventing blood flow completely; regurgitation, where the valve does not seal tightly, allowing backflow of blood; and stenosis, where the valve opening is too small, making the heart work harder to pump blood [12].
Myocardial Disease/Cardiomyopathy	The difficulty of the heart pumping blood increases due to thickened or stiff heart muscle that does not expand, potentially leading to heart failure [4].
LV Dysfunction	The heart pumps weakly due to a variety of issues including hypertension, diabetes, and kidney disease [23].
Congenital Heart Disease	There are one or more defects with the heart structure at birth which affect the way that blood flows through the heart [31]. These issues can include valve defects, holes in the chamber walls, or excess heart tissue in passages [31].
Abnormal Cardiac Output	There is a decreased blood flow to organs in the body due to a decreased cardiac output, due to low blood volume, heart damage, or aortic stenosis [7].

These conditions are fairly common and cardiac catheterization is an important step in addressing what the root cause of the issues is.

During cardiac catheterization, some difficulties arise due to the constant motion of the heart. Navigating through veins while the heart is beating is no easy feat, with visual difficulties from the opaque quality of blood and the tissue walls moving as cardiac muscle contracts [10]. Ultrasound imaging is beneficial for overcoming these difficulties, eliminating the obscuration of the lumens of the veins. Additionally, controlling the forces applied to the vein walls is an obstacle to steering of the catheter in order to avoid damaging veins as the catheter moves through the body [10]. Without a catheter steering system, the judgment and expertise of a clinician becomes extremely important during navigation. On top of these navigation difficulties, when using internal imaging it can be difficult to position the catheter tip in the correct orientation to view the veins ahead.

1.3 Mechanical

1.3.1 Kinematics

The mechanics of a catheter is controlled through manipulation of tension and torque on wires attached to the distal catheter tip. The pull wires run from the control knobs on the handle

through the shaft to the catheter tip. By pulling specific wires, different segments of the distal shaft can be manipulated. The degrees of freedom (DOF) for a mechanically steered catheter is determined by the number of steerable segments and number of wires the device is made of. A catheter tip with one DOF will have two wires running parallel from the catheter tip through the distal shaft to the handle. To manipulate the device one wire will be put in tension while the other wire is slack, allowing movement in a single plane [33]. Every additional pair of guide wires will add an additional DOF by allowing movement in a new plane as shown in Figure 4.

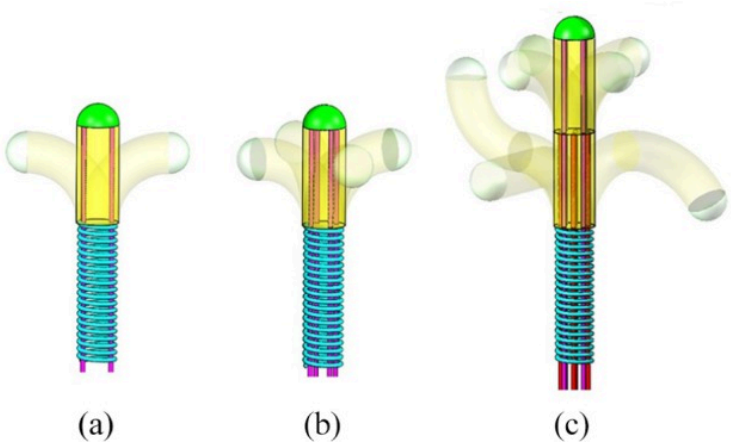

Figure 4: Degrees of freedom for steerable catheter tips (a) One DOF in a single steering segment (b) Two DOF in a single steering segment (c) Multiple DOF with two steering segments [1].

A IVUS catheter typically has two degrees of freedom in the distal shaft allowing movement in the X and Y planes (pitch and yaw). Along with bending in the distal shaft the catheter handle has two DOF on the Z axis, roll and translate. Twisting the handle will apply counterclockwise or clockwise torque on the proximal shaft, rotating the catheter about the Z axis. Shaft shortening can occur when the torsion energy applied to the handle does not reach the tip of the catheter due to low proximal shaft stiffness [1]. Shaft shortening can result in limited catheter tip movement making the device less precise. Additionally, force applied on the handle to create translational movement along the Z axis controls the forward and backward motion of the device.

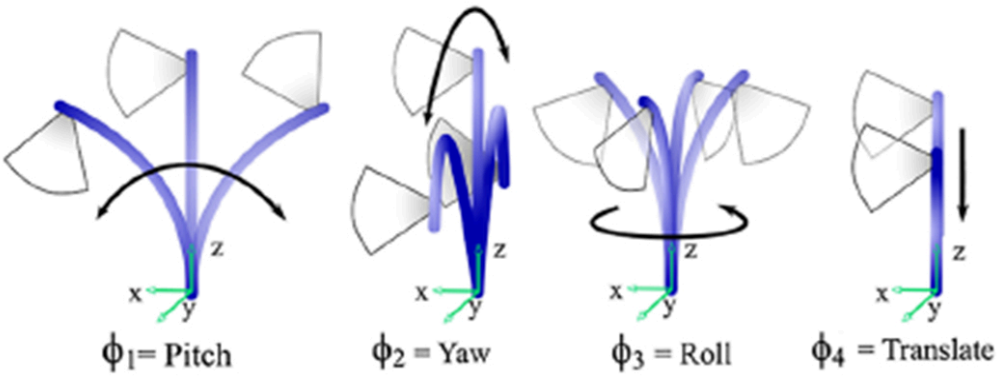

Figure 5: Ranges of motion for the catheter tip and distal shaft of an IVUS Catheter [24].

During cardiac catheter procedures, a physician would apply force on the handle to propel the device forward while manipulating the control knobs to steer the distal tip in a desired direction [24]. The addition of a second steering segment in the distal shaft would increase the DOF a device could manipulate.

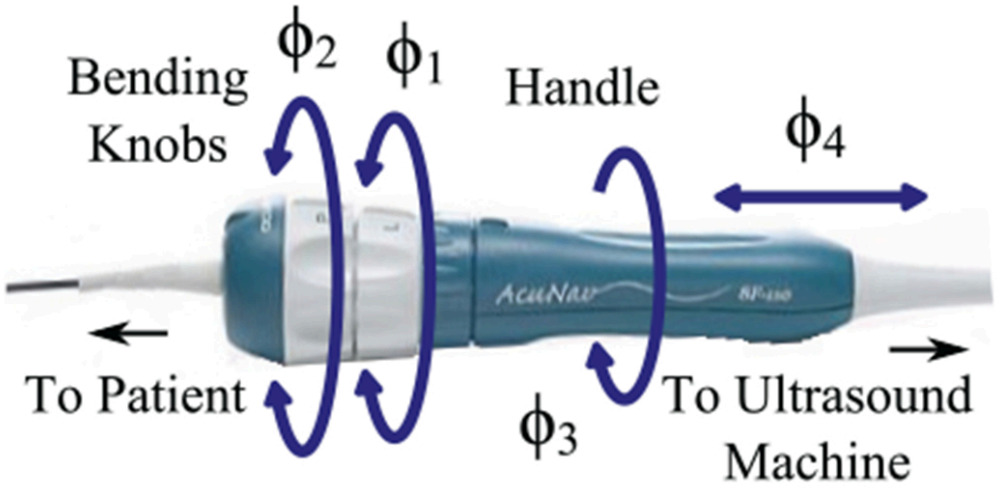

Figure 6: IVUS catheter handle with degrees of freedom illustrated [24].

Kinematics can also be used to calculate the position of the catheter, specifically forward and inverse kinematics. Forward kinematic calculations use the joint angles and angular velocities of the robot arm to determine the position and velocity of the end-effector, or the tip of the robot [28]. Inverse kinematics uses the known position of the end-effector to calculate the joint angles and angular velocities of the robotic arm. Both calculations use the Denavit-Hartenberg method to transform between the joint space (a vector whose components are translational of robotic arm joints [23]) $[q_1, q_2, \ldots q_n]$ and the task space (the position of the end effector [32]) [z, y, z, psi, theta, phi]. The most common method of Denavit-Hartenberg uses four parameters (a_{i-1}, α_{i-1}, d_i, θ_i). These parameters represent link length, link twist, link offset and joint angle. Each joint on a manipulator is defined by either a prismatic or revolute joint where prismatic joints are translational and revolute joints are rotational. Below is the coordinate frame assignment of a general manipulator.

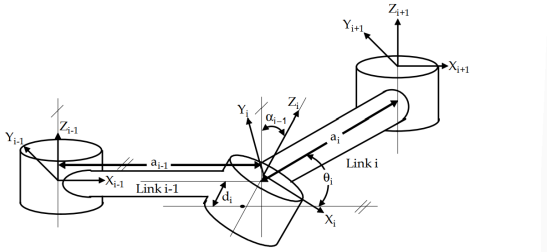

Figure 7: The coordinate frame assignment of a general manipulator [32].

The general transformation matrix ${}^{i-1}_{i}T$ for a single link is:

$$
\begin{aligned}
{}^{i-1}_{i}T &= R_x(\alpha_{i-1})D_x(a_{i-1})R_z(\theta_i)Q_i(d_i) \\
&= \begin{bmatrix} 1 & 0 & 0 & 0 \\ 0 & c\alpha_{i-1} & -s\alpha_{i-1} & 0 \\ 0 & s\alpha_{i-1} & c\alpha_{i-1} & 0 \\ 0 & 0 & 0 & 1 \end{bmatrix}\begin{bmatrix} 1 & 0 & 0 & a_{i-1} \\ 0 & 1 & 0 & 0 \\ 0 & 0 & 1 & 0 \\ 0 & 0 & 0 & 1 \end{bmatrix}\begin{bmatrix} c\theta_i & -s\theta_i & 0 & 0 \\ s\theta_i & c\theta_i & 0 & 0 \\ 0 & 0 & 1 & 0 \\ 0 & 0 & 0 & 1 \end{bmatrix}\begin{bmatrix} 1 & 0 & 0 & 0 \\ 0 & 1 & 0 & 0 \\ 0 & 0 & 1 & d_i \\ 0 & 0 & 0 & 1 \end{bmatrix} \\
&= \begin{bmatrix} c\theta_i & -s\theta_i & 0 & a_{i-1} \\ s\theta_i c\alpha_{i-1} & c\theta_i c\alpha_{i-1} & -s\alpha_{i-1} & -s\alpha_{i-1}d_i \\ s\theta_i s\alpha_{i-1} & c\theta_i s\alpha_{i-1} & c\alpha_{i-1} & c\alpha_{i-1}d_i \\ 0 & 0 & 0 & 1 \end{bmatrix}
\end{aligned}
$$

Figure 8: The general transformation matrix for a single link

The first three matrices represent its orientation and the last its position. In order to get the forward kinematics of the end-effector with respect to the base frame, the T matrices for each link are multiplied together

$$
{}^{base}_{end\_effector}T = {}^{0}_{1}T\,{}^{1}_{2}T \ldots {}^{n-1}_{n}T
$$

Inververse kinematics can be solved in two different ways, the geometric and algebraic approach. The geometric approach works by decomposing the geometry of the manipulator into several planes. This approach is applied to more simple robotics. Below is an example of a manipulator and the equations derived from its geometry.

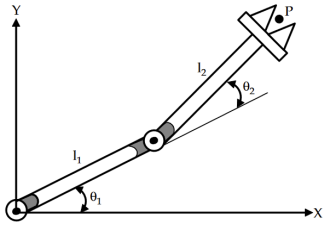

$$p_x = l_1 c\theta_1 + l_2 c\theta_{12}$$

$$p_y = l_1 s\theta_1 + l_2 s\theta_{12}$$

Figure 9: Example manipulator [32].

For manipulators with more complex structures, the algebraic approach is applied. The equation to find the inverse kinematics using the algebraic approach is:

$$
{}^{0}_{6}T = \begin{bmatrix} r_{11} & r_{12} & r_{13} & p_x \\ r_{21} & r_{22} & r_{23} & p_y \\ r_{31} & r_{32} & r_{33} & p_z \\ 0 & 0 & 0 & 1 \end{bmatrix} = {}^{0}_{1}T(q_1)\,{}^{1}_{2}T(q_2)\,{}^{2}_{3}T(q_3)\,{}^{3}_{4}T(q_4)\,{}^{4}_{5}T(q_5)\,{}^{5}_{6}T(q_6)
$$

To find the inverse kinematics solution for the joint q_1 as a function of its known elements, each side of the equation can be multiplied by an identity matrix. This turns the above equation into

$$\left[{}^{0}_{1}T(q_1)\right]^{-1}\ {}^{0}_{6}T = {}^{1}_{2}T(q_2)\ {}^{2}_{3}T(q_3)\ {}^{3}_{4}T(q_4)\ {}^{4}_{5}T(q_5)\ {}^{5}_{6}T(q_6)$$

This equation can be derived for every other joint to create a system of equations. q_1 can now be solved as a function of the other variables. Once this is found the other joint variables can be solved for.

The DH parameters can be applied to catheter systems. Below is a catheter and its table of DH parameters.

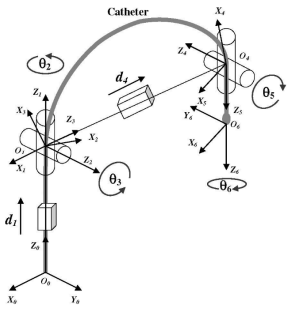

TABLE I
MODIFIED D-H TABLE

Link	a	α	d	θ	Joint variable
1	0	0	d_1	0	d_1
2	0	$\pi/2$	0	θ_2	θ_2
3	0	$\pi/2$	0	$\pi/2+\theta_3$	θ_3
4	0	$\pi/2$	d_4	0	d_4
5	0	$\pi/2$	0	$\pi+\theta_5$	θ_5
6	0	$\pi/2$	0	θ_6	θ_6
-	0	0	d_7	0	-

The distal end is unnumbered.

Figure 10: Catheter DH parameters [32]

In this diagram,O_0 - O_1 represents the base of the distal staff. This is shown in the diagram as a singular prismatic joint. O_1 - O_4 represents the bending section of the distal staff. Thai is represented by two revolute joints and one prismatic joint. Lastly, O_4 - O_6 represents the distal end of the catheter. This part of the catheter is almost rigid meaning the length of this section is a constant. Using forward kinematics, the transformation matrix for this system is found to be:

$$T_0^7 = \left[\begin{array}{ccc|c} c\theta_2^2 c2\theta_3 - s\theta_2^2 & c\theta_2 s2\theta_3 & -c\theta_3^2 s2\theta_2 & c\theta_2(d_4 c\theta_3 + d_7 s2\theta_3) \\ c\theta_3^2 s2\theta_2 & s\theta_2 s2\theta_3 & -s\theta_2^2 c2\theta_3 + c\theta_2^2 & s\theta_2(d_4 c\theta_3 + d_7 s2\theta_3) \\ c\theta_2 s2\theta_3 & -c2\theta_3 & -s\theta_2 c2\theta_3 & d_1 + d_4 s\theta_3 - d_7 c2\theta_3 \\ \hline 0 & 0 & 0 & 1 \end{array}\right]$$

1.4 Robotic

1.4.1 Algorithms

The main difference between mechanically driven intracardiac steering systems and robotic intracardiac steering systems is the use of neural networks. A neural network is a subset of machine learning that simulates the human brain [3]. Neural networks are the backbone of machine learning algorithms, and they are useful for pattern recognition, classification, and predictive analysis [3]. Robotic intracardiac catheter steering systems use a multitude of deep learning algorithms to steer the robot in the correct direction.

1.4.2 Proportional-Integral-Derivative (PID) Controller

PID controllers are used alongside sensors to control the output of a system. These controllers are closed loop systems, meaning the system uses feedback to control the state of the system. As seen in Figure 11, which is an example PID controller of a robotic manipulator actuated by the tendon sheath, the input of the controller (highlighted in green) is the difference between the desired and actual value of the robotic arm [21]. The output of the controller is calculated as seen in Figure 12, where Kp is the proportional coefficient, Ki is the integral time constant, and Kd is the differential time constant [21]. The proportional, integral, and derivative coefficients are determined based on experimentation of the controller [21].

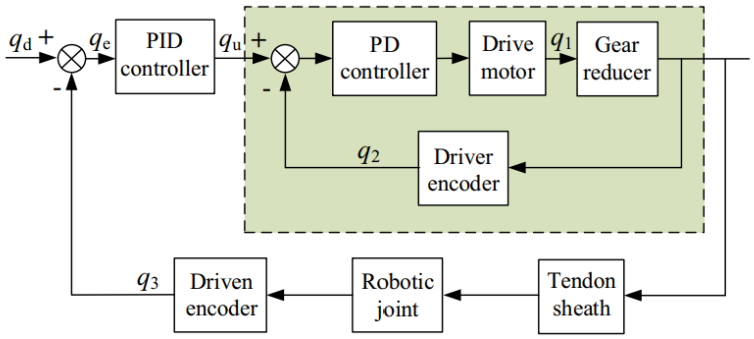

Figure 11: Standard PID controller [17]

$$q_u(t) = K_p\left[q_e(t) + \int_0^t \frac{q_e(t)}{K_i}dt + \frac{K_d dq_e(t)}{dt}\right]$$

Figure 12: Calculation of output signal of the controller

Despite its advantages, using a PID controller in a complex system with multiple variables to control can be time consuming [21].

1.4.3 Position Tracking

1.4.3.1 Step Counts

One of the biggest advantages of using a stepper motor is its ability to achieve precise positioning [13]. To calculate the position of the stepper motor in relation to the angle, theta, the following equation can be used:

$$\Theta = n * \boldsymbol{\alpha} \text{ (Eq.1)}$$

Where theta is the the position of the motor in degrees, n is the number of steps, and $\boldsymbol{\alpha}$ is the motor step angle. The step angle can be found in the specifications sheet for the particular stepper motor.

1.4.3.2 External Camera

One method is force control, which completes a transformation on the tip force to calculate the configuration [9]. Through the force measurement, this algorithm is able to calculate the position and use inverse kinematics to drive the actuators [9]. Another method is the control-LSTM method, which can predict commands that reduce the force on the actuator tip [9]. By using these two algorithms, the end effector (tip) of the robot can be controlled in a way that minimizes damage to the tissue.

One study was done using a position tracking algorithm called "You Only Look Once" (YOLO). YOLO is an object detection algorithm that processes images at an incredibly fast rate using neural networks. YOLO works first by dividing up an image into a grid. Each grid cell is processed as its own image. In each image, YOLO looks for objects of a certain class, the objects it is trained to find. For each grid cell YOLO returns a vector. This vector holds valuable information such as the centroid of the object in that grid cell, its boundary box, and its classification. These vectors are then used to train the neural network to get more accurate at detecting these images. For the YOLO algorithm there can only be one object per grid cell. If there is more than one, the second object will be ignored. The grid cells need to be sized according to the size of the objects in the image. In this study YOLO was used as a position tracking algorithm to track where the catheter was in the body. The algorithm drew a boundary box to indicate the position of the catheter.

1.4.3.3 Serial Port Communication

A communication protocol is a system of rules that allows data to be transferred from one device to another [8]. Specifically, serial communication is the process of sending data from one device to the other one bit at a time [8]. Serial communication is widely used in industry, as it has a simple architecture and can streamline communication between two microcontrollers [8].

There are two types of communication protocols: Inter-system and Intra-system [8]. The inter-system protocol is used to communicate between two different devices through a bus system [8]. There are three main protocols within the inter-system protocol [8]:

1. UART (Universal Asynchronous Transmitter and Receiver): Serial communication using a receiving and transmission end. Information is transmitted as bytes of data and is received on the receiving end. Examples of this form of communication include emails and text messages.

2. USART (Universal Synchronous and Asynchronous Transmitter and Receiver): This form of communication is similar to UART, but data is transmitted along

with clock pulses. This typically involves setting different baud rates for transmitted messages.

3. USB (Universal Serial Bus): This communication is used to send and receive data to the host through a USB device.

UART communication specifically can be used to communicate information between Arduino and MATLAB. The arduino board acts as a UART transmitter when it sends data over the serial port and MATLAB acts as a serial receiver. Using the print() and read() commands in the Arduino IDE, data can be sent and received. Similarly, MATLAB can also act as a transmitter while the Arduino IDE receives data. A serial object can be created in MATLAB handling data using the commands such as readline() and write(). This communication allows for different processes like motor control and position calculation to be handled by different IDEs.

1.4.4 Mapping Systems

Mapping systems are an integral part of robotic intracardiac catheter systems. There are three main mapping systems that have been explored: the CARTO system, NavX, and Rhythmia.

1. CARTO System [30]

The CARTO system uses magnetic localization to get an (x,y,z) and (roll, pitch, yaw) location of the catheter. To calculate the respiration of the patient, the system tracks the change in impedance readings as the catheter passes through the heart and lungs. These impedance values then translate to the rate of respiration by determining the corresponding voltage change on the same electrodes.

2. NavX System [30]

The NavX System uses a frequency signal that is sent through three patches applied to the skin of the patient on the (x,y,z) planes. This signal creates a voltage across the planes, which creates a three-dimensional position across the electrodes.

3. Rhythmia System [30]

The Rhythmia System uses a small catheter with 64 electrodes to create an electroanatomical map. To create this map, a multitude of algorithms are used in alignment with reference planning to continuously update the location of the catheter.

1.4.5 Chart of Specifications

Table 2: Chart of specifications outlining different catheter robotic systems that exist presently.

System	Mechanical Specifications	Software Specifications	Function/Performance Specifications
Niobe Magnetic Navigation System [30]	- 2 permanent magnets on either side of the patient to produce magnetic field - Catheter contains 3 inner magnets to align parallel to magnetic field	- Capability with CARTO system - Remotely advances catheter by localizing with magnetic field	- Used for ablation (a procedure to treat atrial fibrillation. It uses small burns to cause scarring to break electrical signals that cause irregular heartbeats [15]) of complex arrhythmias such as fibrillation and scar related VT (ventricular tachycardia- a type of abnormal heartbeat that occurs when the lower chamber of the heart beats too fast to pump well and the body doesn't receive enough oxygenated blood [18]) - Unknown whether it makes procedure more efficient in clinical setting - Desire to add additional deflectable sheath (improves catheter stabilization and maintain proper catheter-tissue contact. It also reduces total procedure time and increases rate of successful ablation [20]) to improve outcomes
CGCI Magnetic Navigation System [30]	- 8 electromagnets to create dynamically shaped magnetic fields around the	- Reshaping of magnetic fields produces 3D motion or change in direction of catheter - Integrated with	- Uses electromagnets instead of fixed magnets so the magnetic field can be altered quickly (fraction of a second). This allows the software algorithms to function constantly and

	patient's torso	NavX system	keep the catheter in a stable location - Initial clinical experience is early
Sensei Robotic Navigation System [30]	- Uses 2 steerable sheaths manipulated with a pull wire mechanism carrying a robotic arm fixed to the table	- Robotic arm controlled in control room using 3D joystick - Used in conjunction with NavX and CARTO	- Has already demonstrated clinical feasibility but unsure whether the outcomes are superior to standard manual mapping

2. Methods and Implementation

The team aimed to devise a mechanism with four degrees of freedom to be utilized in IVUS procedures, mimicking the movements of a surgeon. When analyzing the possible solutions, the team had three options to consider. The first option was to create a robotic mechanism to accentuate an existing ICE catheter. The second option was to create a mechanism that would utilize deconstructed components of an ultrasound catheter, similar to current Robotic catheter devices on the market today. The final option was to build upon the second design option but incorporate a custom catheter tip adding an extra 2 DOF to the catheter. The team opted to utilize the first design option since surgeons are trained to use this catheter for various cardiac procedures, enabling them to intervene easily if the autonomous system were to fail. By choosing this option the team also made it more accessible using a product hospitals already have.

To create a remote intracardiac catheter steering device using an existing ultrasound ICE catheter the team outlined key objectives. Originally the plan was to make the device fully autonomous including trajectory planning however the objectives were altered due to time constraints. The figures below outline the key objectives and the revised objectives.

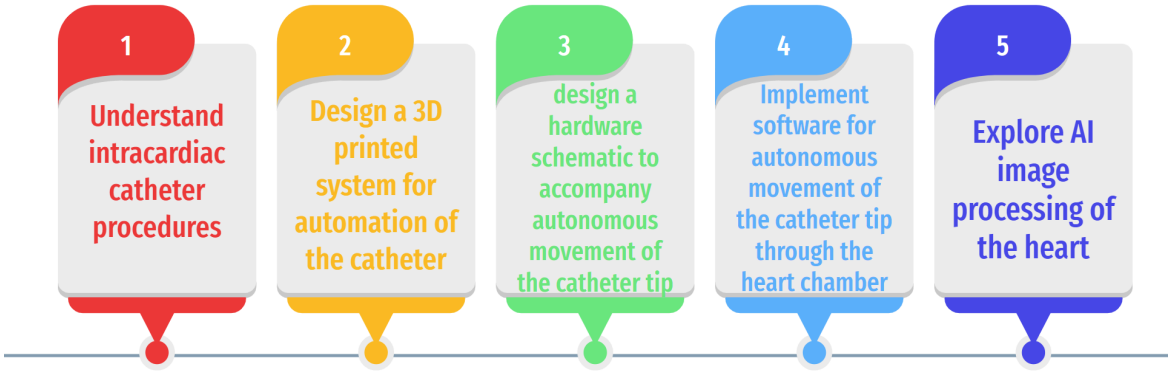

Figure 13: Objectives set at the beginning of A-term

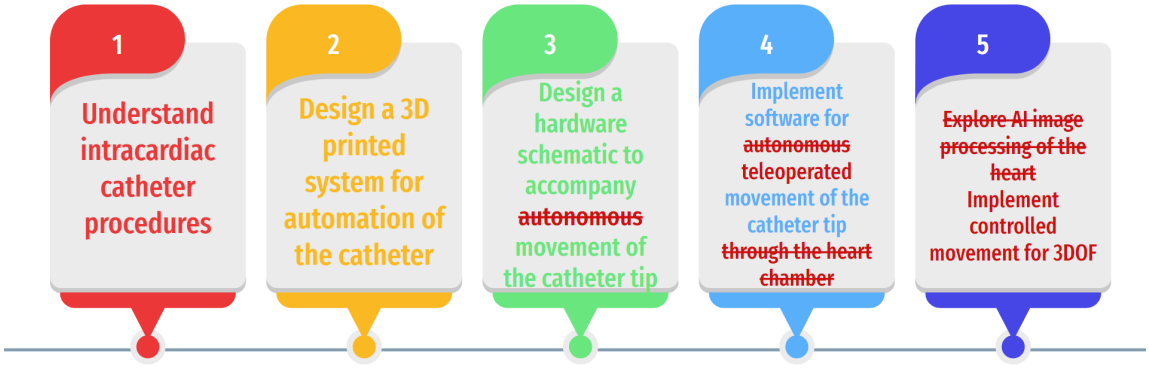

Figure 14: Revision of goals

Over the course of three terms the team has completed three iterations of the device. The first iteration focuses on designing mechanisms to control the rotational, translational, and directional movement of an ICE catheter. For the second iteration, edits were made to finalize designs and initial modeling and assembly in solidworks began. The third iteration focused on assembly of directional components along with minor adjustments to designs. The following sections will address all three iterations according to mechanical, hardware, and software components.

2.1 Iteration 1

2.1.1 Mechanical

A thorough inspection on the mechanics of the ice catheter highlighted the four key movements the robotic device must produce: 270° degree rotation of knobs 1 and 2, 360° degree rotation of the catheter handle, and translational movement of the catheter wire. Important measurements were taken for rough sketch designs as shown in Figure 15 below.

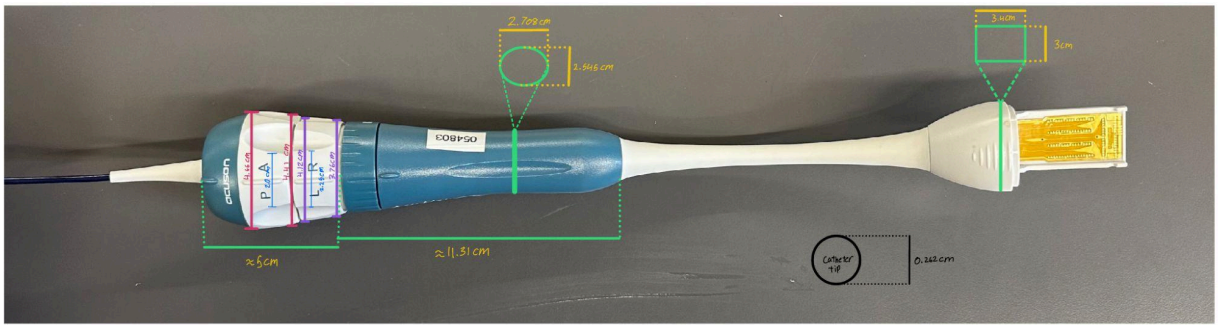

Figure 15: ICE catheter with drawn dimensions.

After analyzing the device, the team was able to compile sketches to actuate the 4 key components. The ICE catheter would be secured into a cylinder cage that would rotate with the help of 2 ball bearings, one on either end, and motor. Each knob would have a gear around it designed to fit the curvature of the device. The team came up with a novel concept to control the translational movement of the catheter wire using omni wheels. Two omnidirectional wheels would be secured to stands horizontally with the catheter wire fed between the wheels. This design would allow the catheter wire to be gripped enough to provide translational movement without hindering the rotational movement with excessive friction. The image below illustrates the team's design plan for future steps.

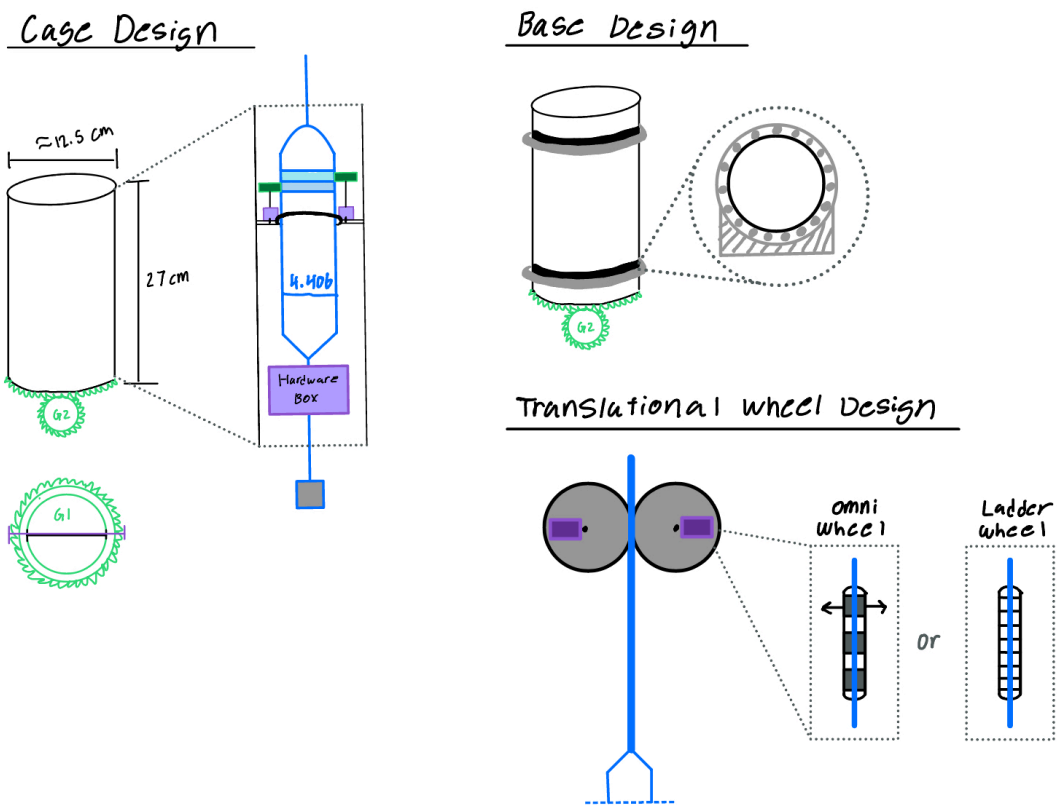

Figure 16: Sketches of chosen design for the robotic catheter device at the end of A term.

For imaging, the team planned to keep the existing ultrasound capabilities at the tip of the catheter for internal imaging during surgery as well as in assisting with the location of the catheter end effector. Additionally, the team planned to implement external ultrasound imaging for clarity of images as well as for a second location for determining the catheter tip pose using kinematics algorithms.

2.1.2 Hardware

The first iteration of the hardware design incorporated an ESP to communicate step counts to each motor. After reviewing this design, the team decided to use multiple ESPs to communicate step counts. This change was made because the mechanical design included a rotational component of the entire system, but with one ESP the wires would get tangled. With multiple ESPs, there would be one for the motor that rotates the whole device, one for the two gears inside of the casing, and one for the two motors that control the translational motion of the catheter. These ESPs will be connected via ethernet to reduce the risk of bad connection that could happen if they were connected with Wi-Fi. With all the boards connected to the ethernet they can communicate with each other allowing them to run in parallel.

2.1.3 Software

In the initial stages, the team decided that MATLAB would be the best software to use to ensure our code ran smoothly. When looking into the ultrasound machine that would be used, the team found that this machine was also running MATLAB. Using MATLAB for the project will allow the team to more easily gather and interpret data from the ultrasound machine. If a different software was used, the team would have to figure out how to transfer the images from the ultrasound to the other software. MATLAB is also a useful tool for matrix math, which is important when calculating trajectories.

2.2 Iteration 2

2.2.1 Mechanical

The second iteration focused on initial modeling and assembly along with alterations to the initial design. Alterations to the initial design took place after some important measurements were collected at the beginning of the term such as torque requirements and surface curvatures on the catheter. The team decided to simplify the design by replacing the bulk cage with two separated cuffs that snuggly hold the catheter within the ball bearings.

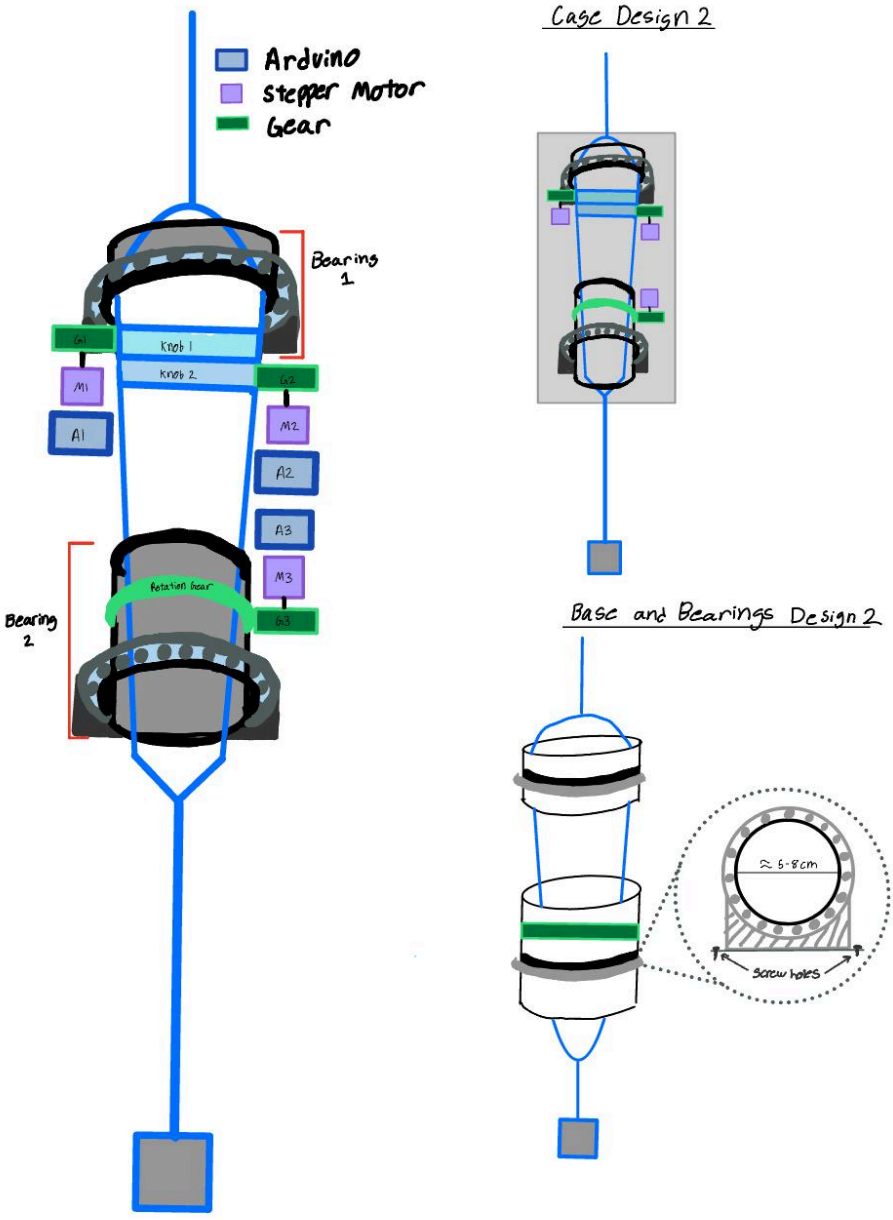

Figure 17: Assembly drawing with dimensions.

The team faced some challenges with the design of the second cuff that attached the catheter handle to the inner track of the ball bearings. The catheter has an asymmetrical, irregular shape, therefore the oval shape that it was estimated as was not a tight enough fit for the cuff. In order to accurately control the fine rotational movements of the catheter, these cuffs must fit perfectly with no movement. Initially, the team intended to solve this problem by filing down the inside of the cuff to fit the catheter snugly. Unfortunately, this was more time-consuming than expected and resulted in an irreplicable design and a looser fit than desired. To solve this, a silicone putty was added to the design to encase the catheter, creating a more regular shape to fit the cuffs around.

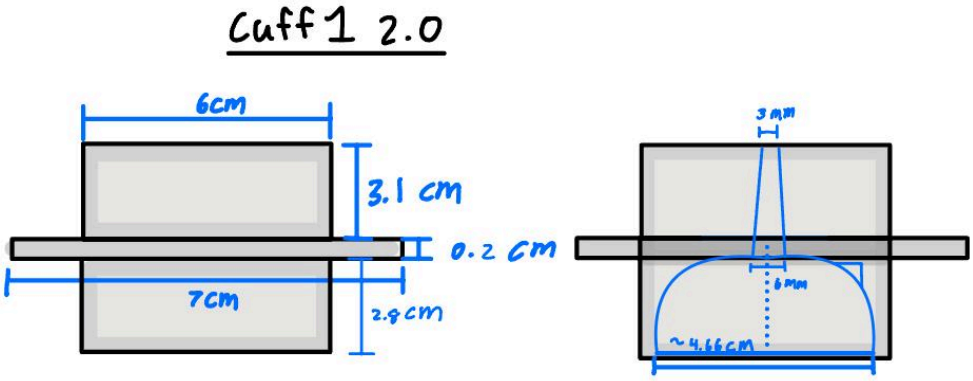

Figure 18: Front cuff drawing with dimensions.

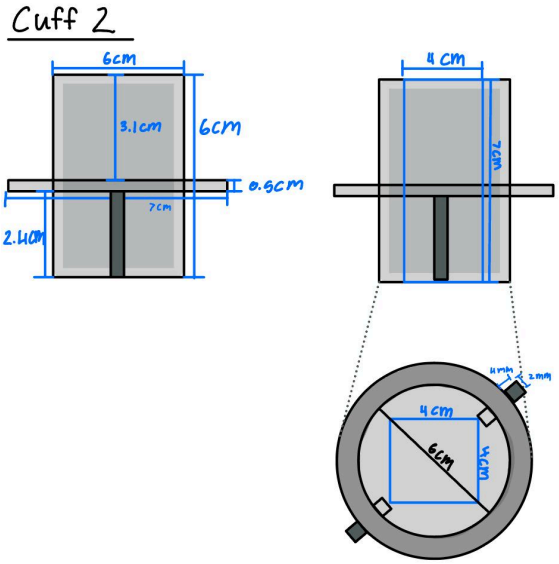

Figure 19: Back cuff drawing with dimensions.

After making adjustments to the drawing the team began modeling components with a computer-aided design made in solidworks. Cuff 1 surrounds the domed top of the catheter, tapering in at the end to snugly fit the tapered wire, as shown in Figure 20. The 2mm ridge

around the exterior of the cuff is used to prevent the cuff from freely sliding through the ball bearing. Additionally a notch cutout was added to the domed part to account for a small ridge on the catheter.

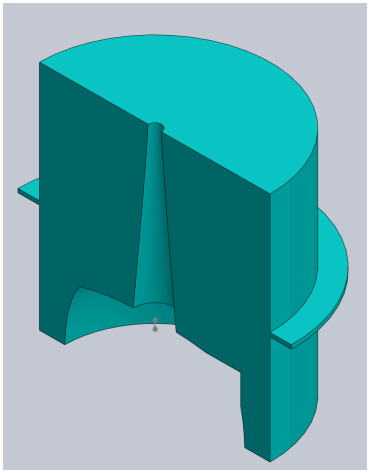

Figure 20: Cross-sectional view of Solidworks model of the front cuff.

The second cuff is broken into two parts with wings containing screw holes to allow the pieces to be secured around the catheter, as shown in Figure 21. A silicone mold encases the handle of the catheter, providing a secure hold on the handle. The silicone mold was made by mixing shower sealant silicone and cornstarch to make a dough and shaped to an outer diameter of approximately 4 cm. The cuffs have an inner diameter of 4 cm and an outer diameter of 7 cm. The screws tighten the back cuff to be a perfect fit on the silicone mold around the catheter handle. There is an external keyed ridge on one side to allow the rotation gear to fit around it securely, which will be explained in more detail later on.

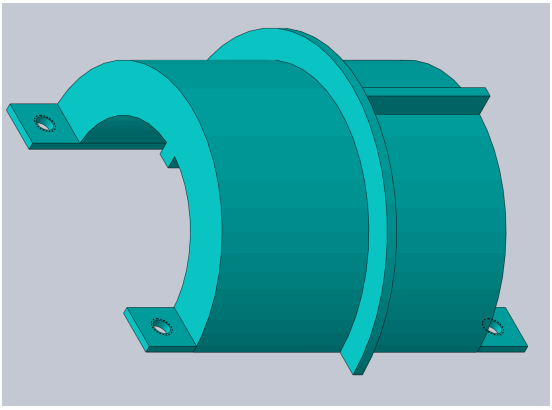

Figure 21: Solidworks model of half of the back cuff.

Next, the knob gears were designed to fit the knobs that control directional bending motion of the catheter tip. These gears were designed to match the sloped shape of the catheter knobs along with a key hole to fit the notch on the catheter knobs, as shown in Figures 22 and 23. The gears have 30 teeth each with a pressure angle of 20° and a Module of 1.

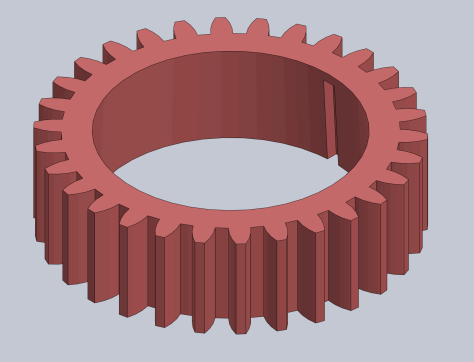

Figure 22: Solidworks model of knob gear 1.

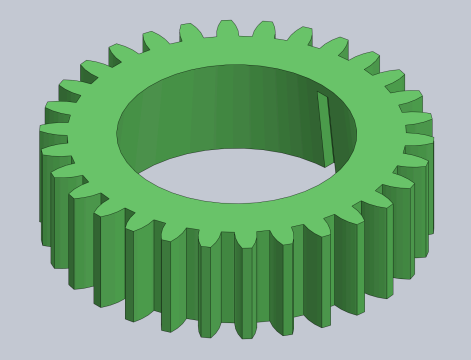

Figure 23: Solidworks model of knob gear 2.

The motor gears were designed so the teeth mesh perfectly with the teeth of the knob gears, as shown in Figure 24. The motor axles cut out on the gears are keyed to fit the stepper motor shafts. The gear teeth were designed to be the same as the knob gears creating a gear ratio of 1.

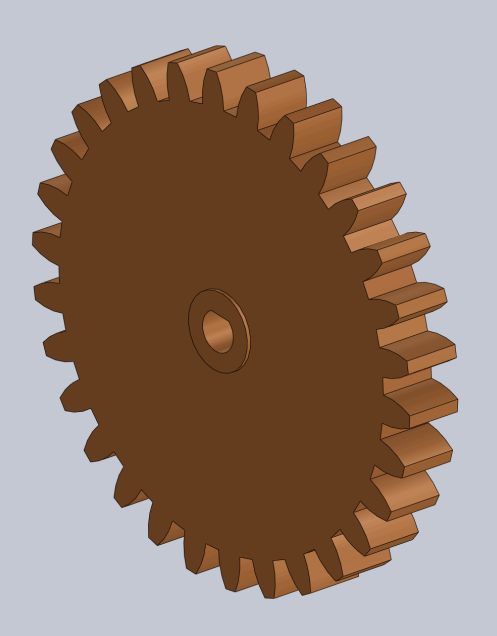

Figure 24: Solidworks model of motor gears.

The rotation gear that controls external rotation of the entire catheter was designed so that the inner diameter fits around the second cuff of the catheter. The ridges on the back of the cuff fit snugly into the keyed notches in the rotation gear, as shown in Figure 25. The rotational gear has 30 teeth and pressure angle of 20° but the module was increased to 2.The motor gears for rotation is a copy of the previous motor gear but the module was edited to be 2 and the number of teeth is 20. The gear in Figure 26 was designed to mesh with the teeth of the rotation gear in Figure 25.

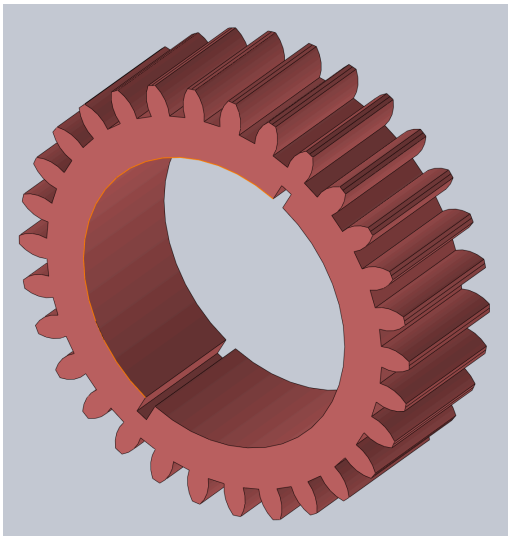

Figure 25: Solidworks model of rotation gear.

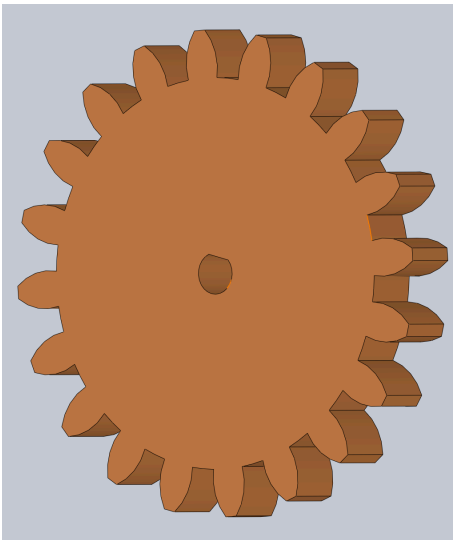

Figure 26: Solidworks model of motor gear for rotation.

Motor stands were designed based on the stepper motors to elevate them to the required level for the motor gears to rotate the knob gears. These stands encase the whole motor with a hole in the front for the motor shaft to fit and screw holes to attach the two sides together, attach them to the board, and attach the encoder cases, as shown in Figure 27.

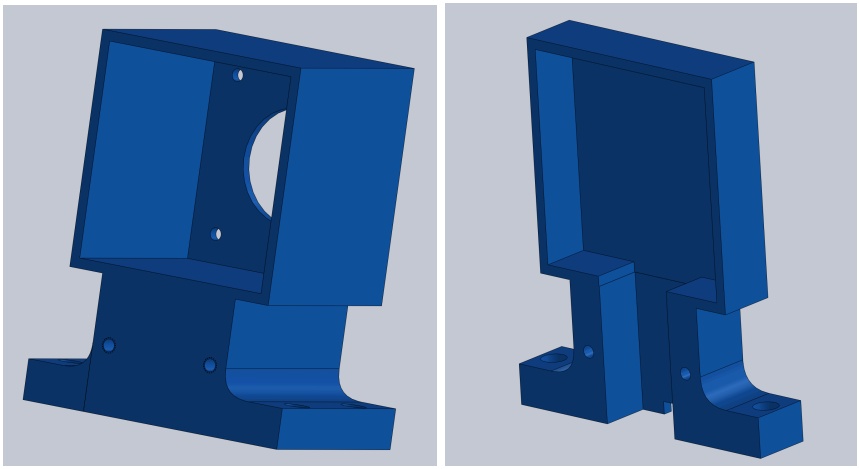

Figure 27: Solidworks model of 55 N-cm motor stand.

The case for the encoder was designed to fit around the encoder and support it, with holes in the top to screw it onto the motor stands. The big hole in the front allows the motor shaft to extend so that the motor gears can attach to it. This case is pictured below in Figure 28.

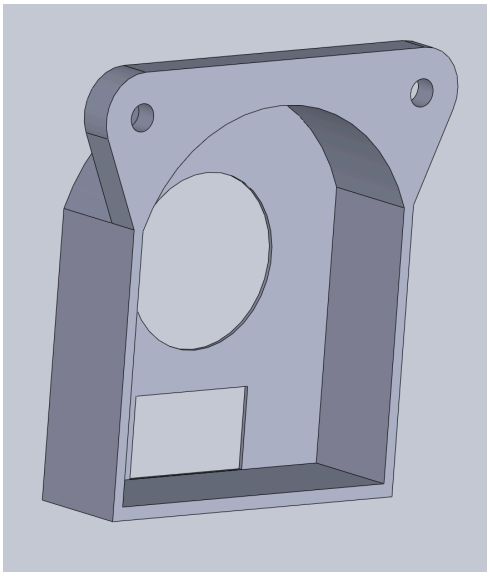

Figure 28: Solidworks model of encoder case.

Each ball bearing has an outer support to keep the device stable and level, encasing the outer tracks of the ball bearings. These have 3 screw holes around the outside that secure the support to the ball bearings, as shown in Figure 29. Additionally, there are holes in the bottom to secure it to the board.

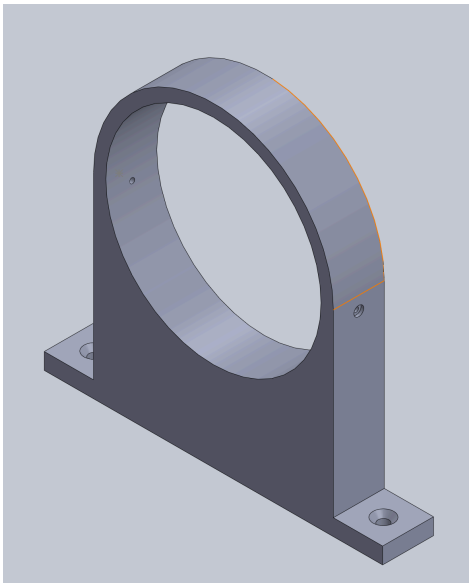

Figure 29: Solidworks model of ball bearings support.

The components above were compiled into a solidworks assembly to ensure proper dimensions and spacing as shown in design assembly in Figures 30 and 31. All the designed pieces were printed in PLA on an Ultimaker 3, and M3 screws are used throughout the design.

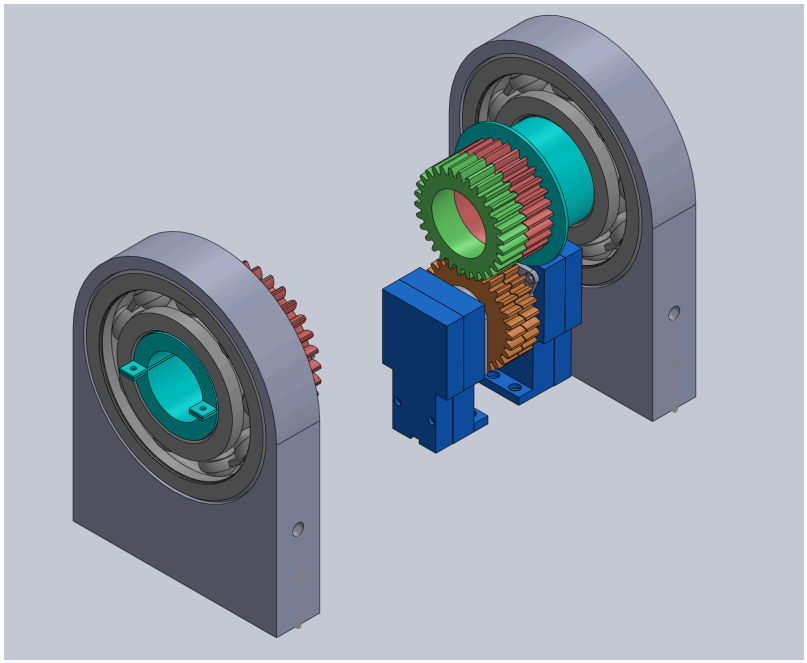

Figure 30: Solidworks assembly of the robotic catheter system.

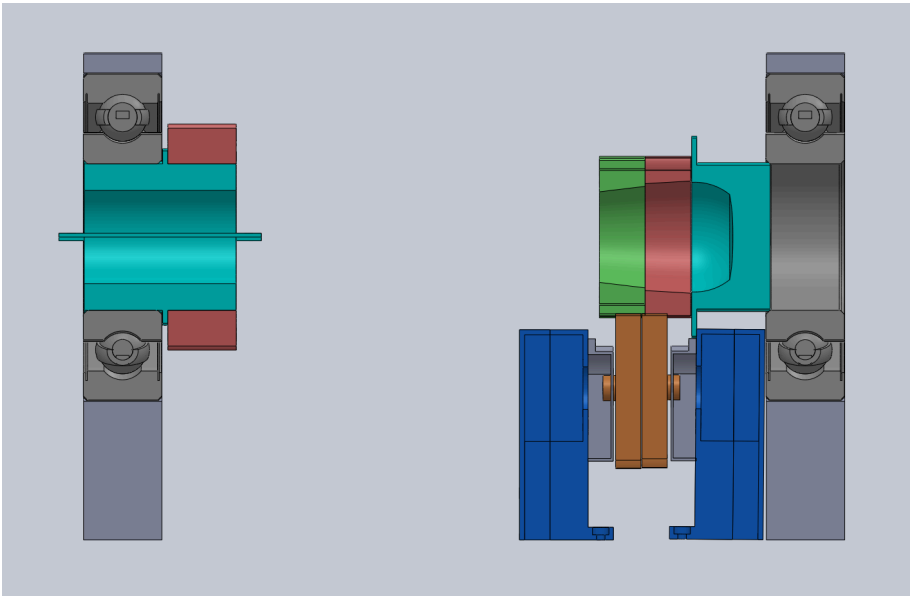

Figure 31: Cross-sectional view of the Solidworks assembly of the robotic catheter system.

Throughout iteration two, adjustments were made to account for unforeseen challenges. In this model, the team edited the knob motor stands to be shorter, and positioned underneath the catheter. This is visible in Figure 31 above. This was intended to create a more stable model with a cleaner design. These stands had to be remodeled due to the lack of encoders in the motors. The team bought separate encoders that were attached onto the shaft of the encoder, and the stands were remodeled to account for this edit, as well as the motor gears. An encasing for the encoder was designed for the revised model.

Additionally, the team ran into the issue with the motors not having enough torque to rotate the knob gears. This may have been due to friction between the gears, increasing the torque required to rotate. Torque measurements were taken using a torque gauge and a 3D printed testing stand shown in Figure 32. Knobs 1 and 2 had a minimum torque requirement of ~7 Ncm to rotate. The 17 N-cm motor was unable to provide the required torque for the knobs, therefore the team replaced the motors with the 55 N-cm motors.

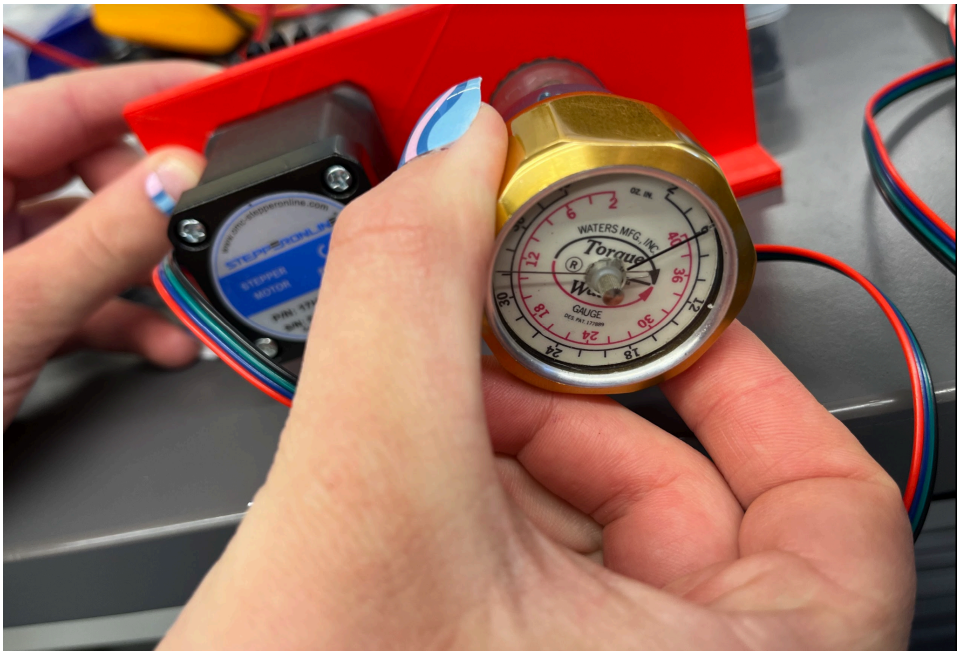

Figure 32: Torque gauge and testing board.

In this iteration, the omni wheels were not finalized yet, but were being designed to provide translational movement. Two sets of two omni wheels would be sandwiched together with a washer in between to create a track between them for the catheter to run through. Each set of omni wheels would be connected to a motor. The team encountered an issue with the texture of the omni wheels. These were expected to be made of a more rubbery material, however they are slick and would not be able to grip the catheter securely. To remedy this, a rubber coating called Plasti Dip was purchased to paint onto the wheels, creating a more adhesive surface. This should allow the wheels to provide translational motion to the catheter.

2.1.2 Hardware

Upon reviewing the design to use multiple ESPs, the team encountered a major learning curve in determining how to connect stepper motors to ESPs. There were no resources on how to connect the devices, but the team concluded through research that using an Arduino would be more compatible with our system.

After switching to an Arduino, the team had to order motor drivers to control the motors. From here, the team was unsure how to track the position of the catheter, as the motors did not have encoder counts. The team then decided to purchase external encoder counts to attach to each motor. The figure below outlines the hardware schematic for this iteration.

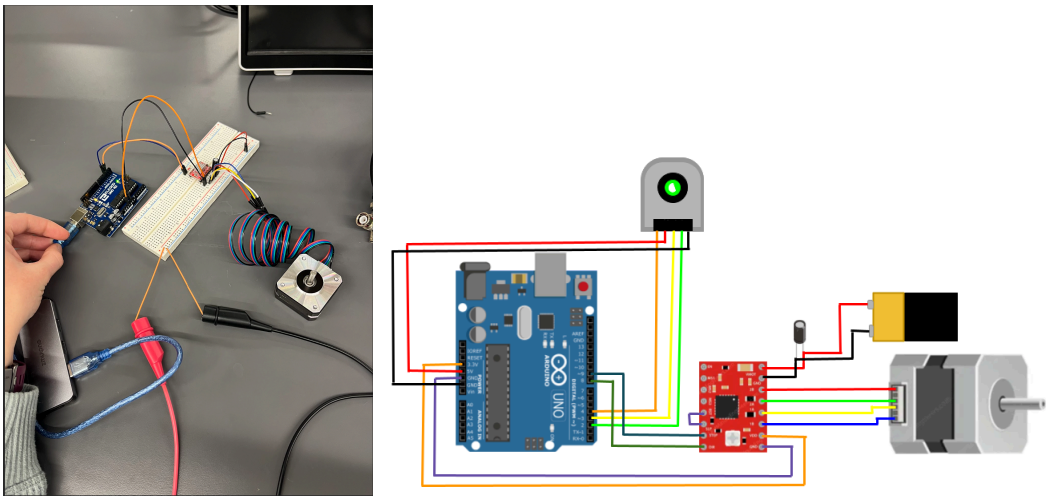

Figure 33: Initial motor setup

2.2.3 Software

The software component of iteration two included simple Arduino code to move the motors. This was also the iteration that the team began implementing simulation code for the validation of results. This is explained in Section 3, Validation of Results.

2.3 Iteration 3

2.3.1 Mechanical

The third iteration focused on manufacturing modeled components and addressing design challenges. After assembling the printed models some issues the team faced were: lack of space, inconsistencies in 3D printing tolerances, and rigidity with the silicone mold.

To address the issue with the motor stands the team decided to move the stands out to the sides of the catheter. As a result, the stands needed to be increased in height and altered the design to be one component with a wire cut out instead of two parts screwed together. The rotational motor remains underneath the catheter to conserve space. These stands can be seen in Figures 34 and 35 below.

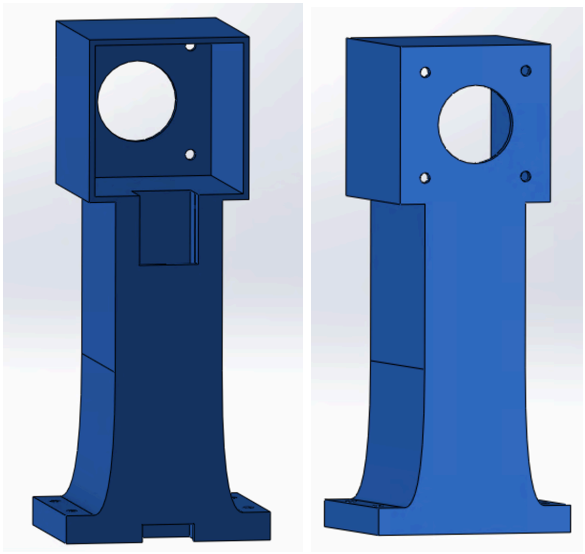

Figure 34: Iteration 3 knob motor stands with built in wire cutout.

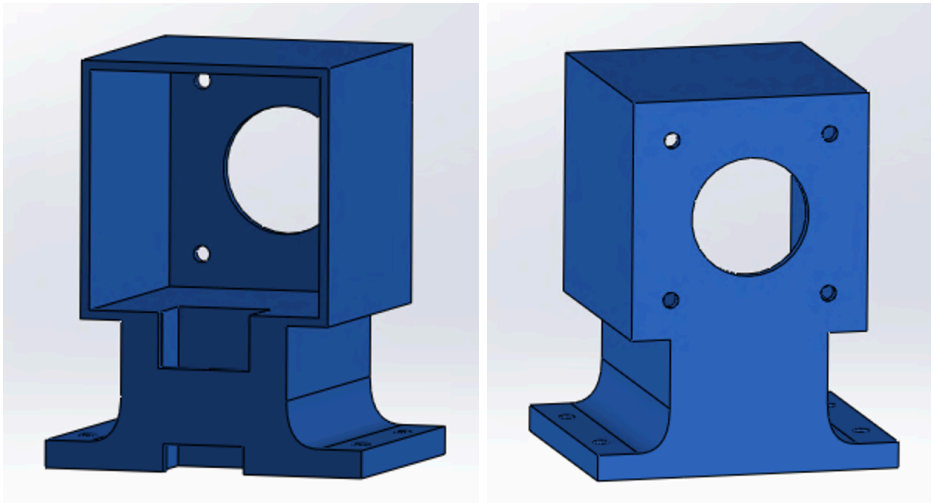

Figure 35: Iteration 3 rotational motor stand.

Due to excess friction between gears increasing the required torque, as mentioned in Section 2.2.1 the team decided to update the motor gears. For this iteration, all motor gears were laser cut on ¼ inch acrylic boards. Laser cutting the gears significantly reduced the friction between abrasive PLA gears and minimized the need for printing tolerances. The laser cutting process for the motor gears is shown on a piece of acrylic in Figure 36.

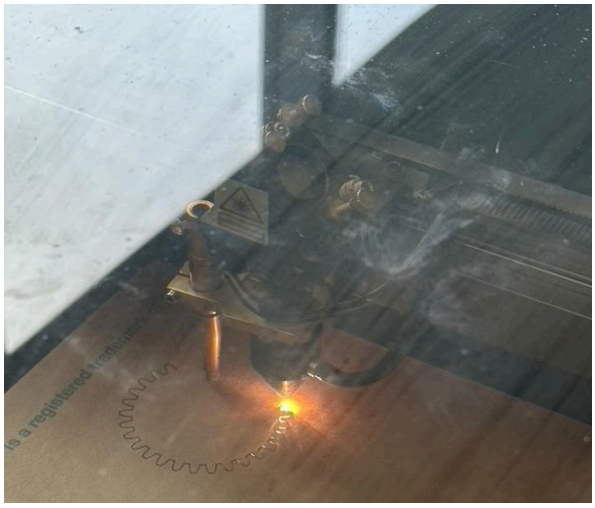

Figure 36: Image of laser cutting motor gears using ¼ in acrylic.

The last adjustment the team made was to upgrade the stiff silicon mold around the catheter handle. The homemade mold stiffened as it dried and shrunk so it no longer fit around the handle of the catheter. The team decided to make a PDMS mold, since PDMS is biocompatible and is used for a variety of engineering purposes due to its electrical and mechanical properties. Unfortunately, the PDMS mold failed, since it was not able to cure in an oven without melting the catheter and 3D printed pieces that encased it. The team implemented a mold using foam gap filler which was able to air dry rapidly. The foam bonded to the cuff, creating a perfectly fitting cuff to encase the catheter handle.

Figures 37-40 depict a Solidworks assembly of the final mechanical system controlling the catheter. The catheter fits into the empty space in the center of this assembly, and the motors will be encased in the motor stands that are displayed. The rotation of the catheter knobs is controlled by the two motors and motor gears positioned to either side of the catheter, while the rotation of the full device is controlled by the motor below the catheter. The red and green gears encase the knobs and are rotated by the orange gears. The red gear around cuff 2 is responsible for the rotational movement along with an orange gear underneath it.

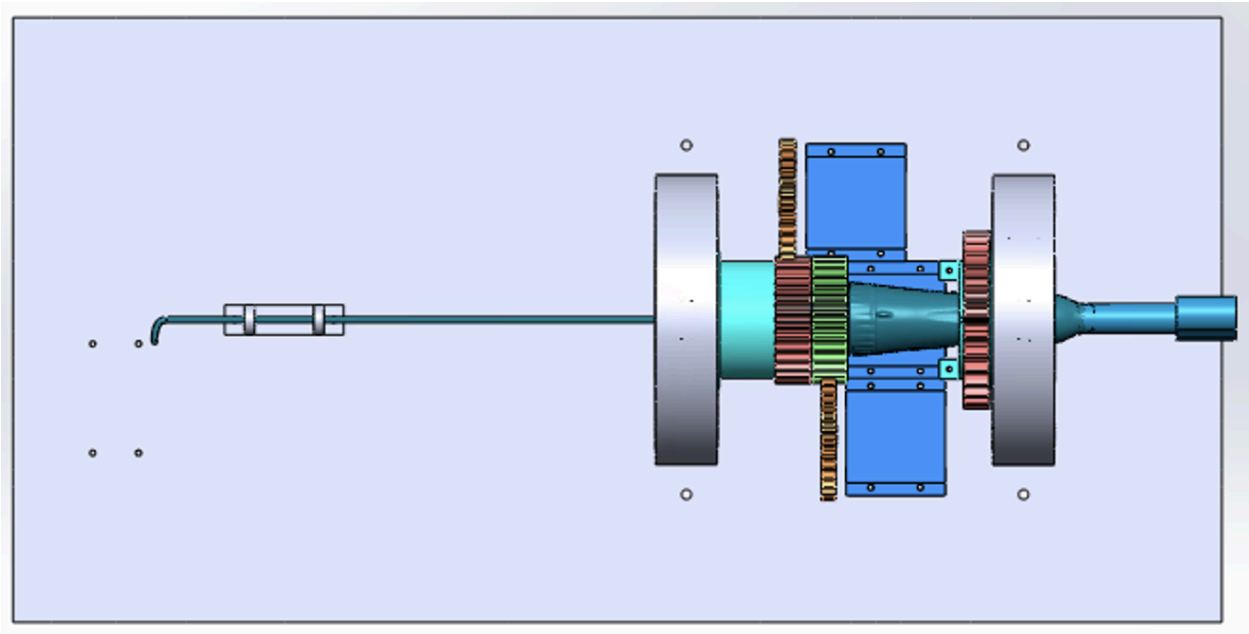

Figure 37: Cross-sectional top-down view of the Solidworks assembly of the robotic catheter system.

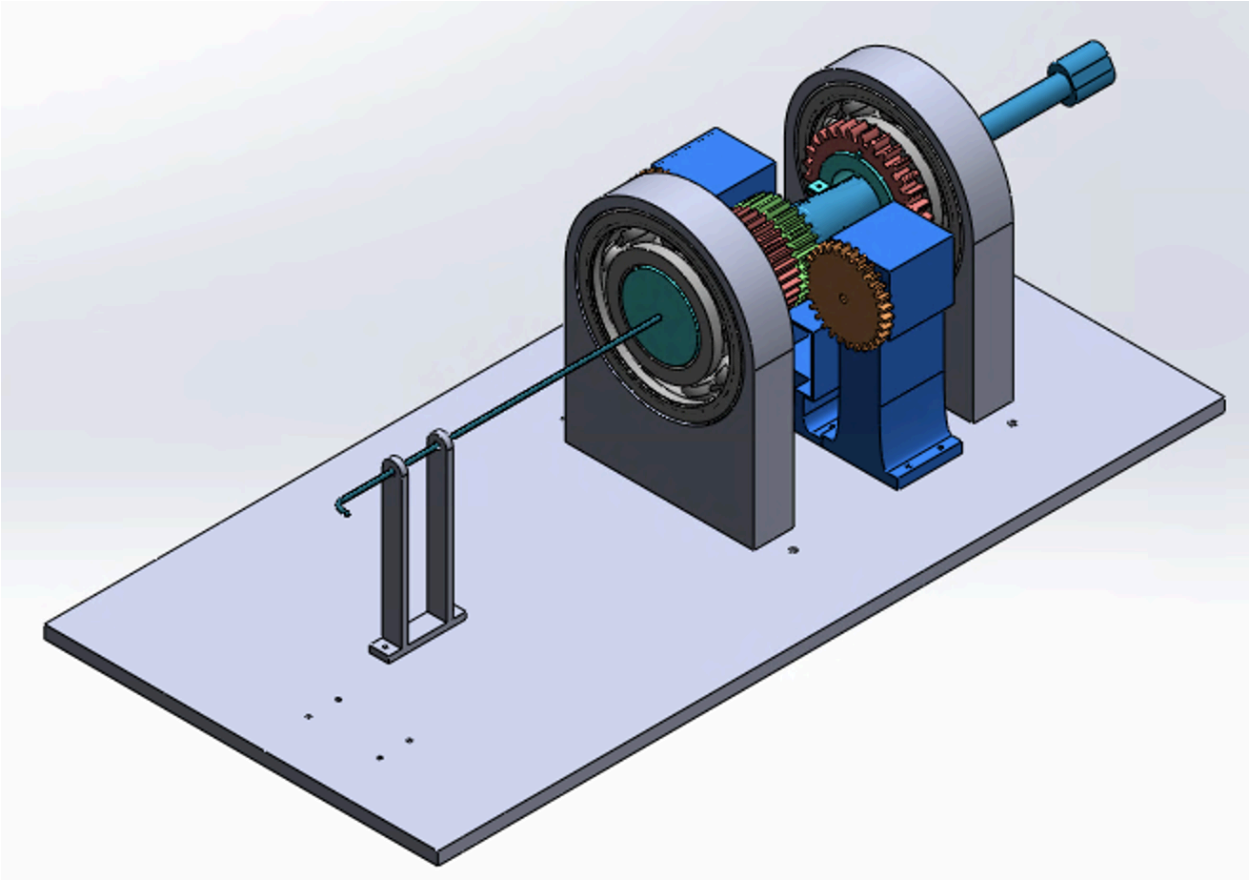

Figure 38: Isometric views of the Solidworks assembly of the robotic catheter system.

The following figures display an exploded view of the robotic steering system to illustrate how the components come together.

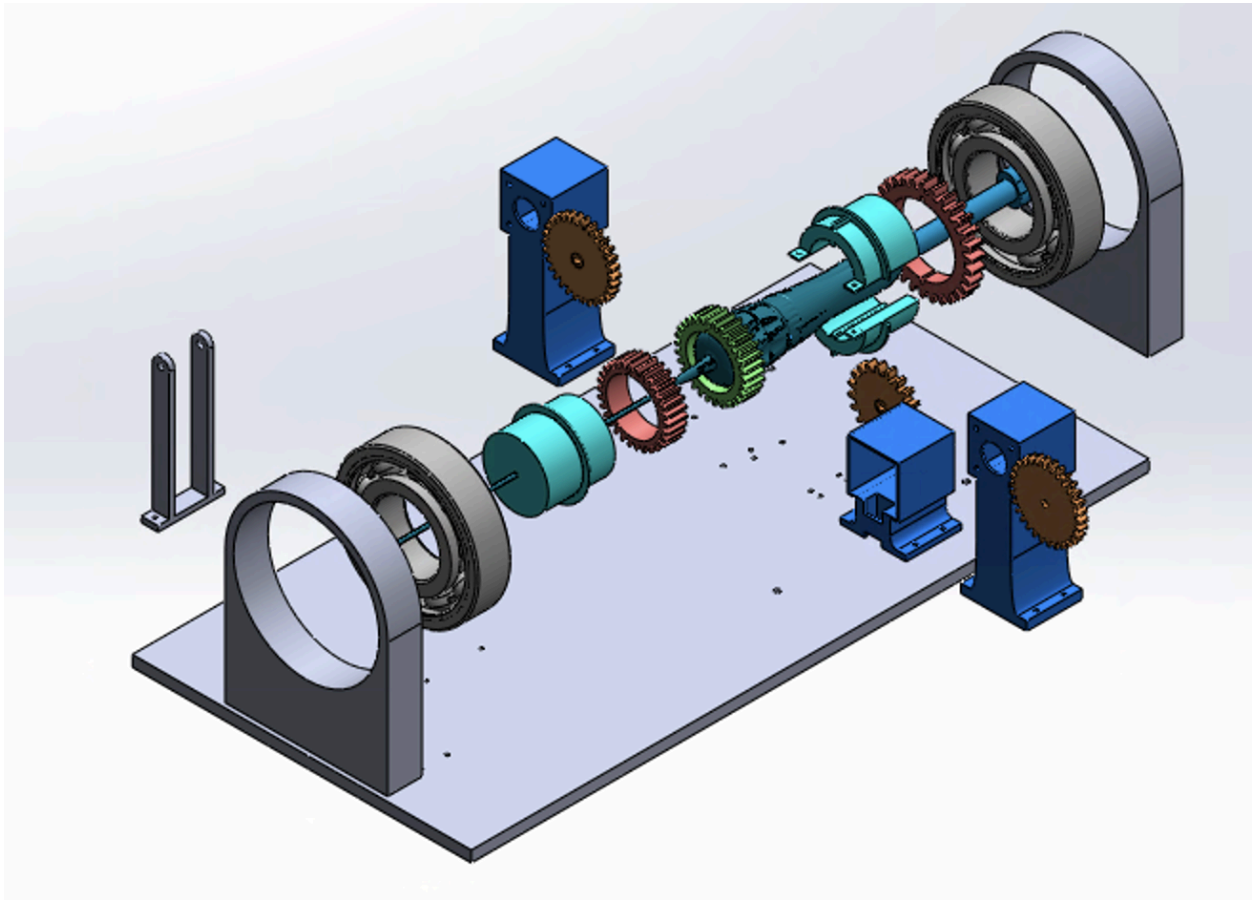

Figure 39: Expanded isometric view of the Solidworks assembly of the robotic catheter system.

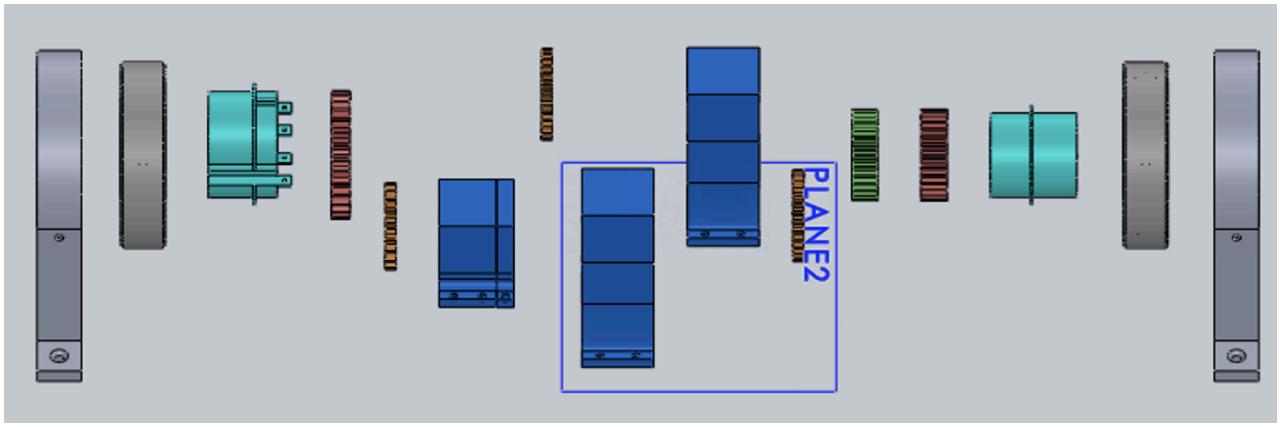

Figure 40: Expanded view of the Solidworks assembly of the robotic catheter system.

2.3.2 Hardware

At the start of the third iteration the team decided to connect all three motors to one arduino to simplify the design. After trying to implement the encoder into the mechanical designs and looking at the encoder code, the team decided that it would be simpler to use step counts. Therefore encoders were completely taken out of the design.

After powering the motors with 9 V in the first two iterations the team realized that the motors weren't generating the max amount of torque. The motors also were not getting all 9 V as the motors were all connected to the same battery. In the latest version of the design each motor is directly powered with 12 V batteries to maximize the torque of the motors.

In the beginning stages of this iteration the team was using potentiometers to control the motors. However, it was challenging to control the motor with these as potentiometers cannot give precise movements. Because of this the team decided to switch to using keyboard commands. There are two keys for each of the three motors, one for clockwise and one for counterclockwise. These motors are controlled using the Arduino microprocessor, which takes in the desired number of steps to move from MATLAB.

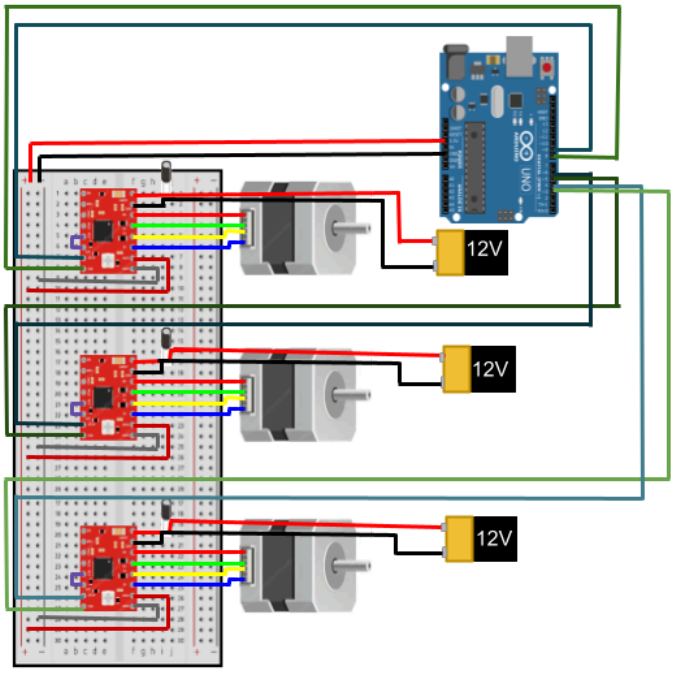

Figure 41: Hardware schematic

2.3.3 Software

One of the first things completed in this iteration was adding the additional motors to the motor code, along with the addition of the AccelStepper library. This library made it easier to control all the motors at once. This library allows the team to set the motors to the same constant speed while being able to write to each motor when needed. As mentioned in the hardware section, each motor is controlled by two keys on the keyboard. This is written in the Arduino IDE as a case statement with each key its own case. When a key is pressed the corresponding motor moves a set amount of steps. Originally, after a key was pressed in the Arduino IDE, the enter key also had to be pressed in order for the motor to move. This meant that the motor could not move continuously. Because of this, the team decided to switch the motor control to MATLAB which allows for a continuous keypress. These keypresses will then be sent to Arduino where it will handle the motor control.

1. Set directional and step pins from Arduino Uno
2. Define variable stepsPerKey which determines how many steps the motor moves when a key is pressed
3. Define variable for the delay between switching the motor from high to low
4. Define variables for step count of each of the motors
5. Define baud rate as 9600 in setup for serial port communication
6. Within a continuous loop:
    a. Read which key is being pressed from the serial port
    b. Set the pin mode and directional to the proper motor based on which key is being pressed
    c. Write the corresponding motor to high voltage
    d. Run the motor within a for loop from zero to the number of steps per key press, delaying by the pre-defined delay rate. This loop will also increase the number of predefined motor steps for that specific motor.
7. Print the motor steps for the selected motor to the serial port for MATLAB visualization

Figure 42: Arduino functionality

To fully implement continuous key press functionality in MATLAB, MATLAB is continuously waiting for a key press while also setting the motor steps to their respective motor variables. In doing this, a physician can continuously press keys and MATLAB will keep track of the number of steps each motor is moving. Keeping track of the motor steps becomes important for the visualization of the catheter movement through simulation in MATLAB.

To visualize the catheter movement in MATLAB, the team needed to derive a robotic model for the catheter.

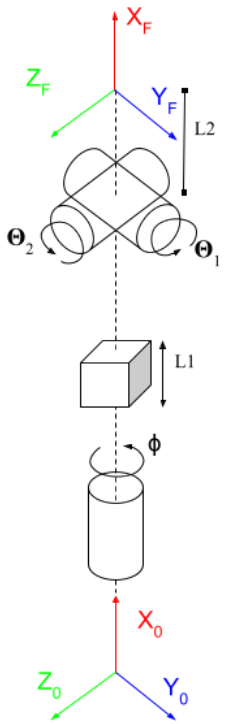

Figure 43: Model of Joints for Steering System

Once the robotic model was derived, the team outlined the DH parameters of the catheter which can be seen in figure 44. These parameters are then used in the forward kinematics calculations to determine the position of the catheter tip when the motors move in a specified amount.

Θ	**d**	**a**	***α***
0	0	0	ϕ
0	0	L_1	0
Θ_1	0	L_2	90
Θ_2	0	L_2	0

Figure 44: DH Parameters for AcuNav ICE Catheter

From these parameters, the team created a script to calculate the homogeneous transformation matrix from the catheter base to the tip. The parameters and equations for the transformation are outlined in Figure 45.

$$T_i^{i+1} = \begin{bmatrix} \cos\theta_i & -\sin\theta_i \cos\alpha_i & \sin\theta_i \sin\alpha_i & a_i\cos\theta_i \\ \sin\theta_i & \cos\theta_i \cos\alpha_i & -\cos\theta_i \sin\alpha_i & a_i\sin\theta_i \\ 0 & \sin\alpha_i & \cos\alpha_i & d_i \\ 0 & 0 & 0 & 1 \end{bmatrix}$$

$$T_0^1 = \begin{matrix} 1 & 0 & 0 & 0 \\ 0 & \text{cosd}(alpha) & -1 * \text{sind}(alpha) & 0 \\ 0 & \text{sind}(alpha) & \text{cosd}(alpha) & 0 \\ 0 & 0 & 0 & 1 \end{matrix}$$

$$T_1^2 = \begin{matrix} 1 & 0 & 0 & L1 \\ 0 & 1 & 0 & 0 \\ 0 & 0 & 1 & 0 \\ 0 & 0 & 0 & 1 \end{matrix}$$

$$T_2^3 = \begin{matrix} \text{cosd(theta1)} & 0 & -1 * \text{cosd(theta1)} & L2 * cosd(theta1) \\ \text{sind(theta1)} & 0 & -1 * cosd(theta1) & L2 * sind(theta1) \\ 0 & 1 & 0 & 0 \\ 0 & 0 & 0 & 1 \end{matrix}$$

$$T_3^4 = \begin{matrix} \text{cosd(theta2)} & -1 * sind(theta2) & 0 & L2 * cosd(theta2) \\ \text{sind(theta2)} & \text{cosd(theta2)} & 0 & L2 * sind(theta2) \\ 0 & 0 & 1 & 0 \\ 0 & 0 & 0 & 1 \end{matrix}$$

$$T_0^4 = T_0^1 * T_1^2 * T_2^3 * T_3^4$$

Figure 45: Transformation matrices for ICE Catheter

Given the step input from the serial port, the MATLAB code is able to take this count and apply it to our forward kinematics function. The model class contains a function that continuously waits for a key to be pressed. Upon receiving a key press, this function reads the number of motor steps printed to the serial port from Arduino, converts these step counts to degrees and centimeters, and inputs these into the forward kinematics function. These represent the values for theta1, theta2, phi, and L1. To convert the step counts to degrees, the team altered the predetermined number of steps per degree of rotation located in the data sheet for the motors. With the gears attached and in contact with the cuff knobs, the team determined the angle at which the catheter tip bends with respect to the motion of the motor is one tenth of what the data sheet suggested. The team accounted for this in the conversion from motor steps to degrees.

After converting from motor steps to degrees, the method waiting for the key input sends those values to the robot class where the kinematics of the catheter is calculated and calls the function to plot the catheter vector in real time.

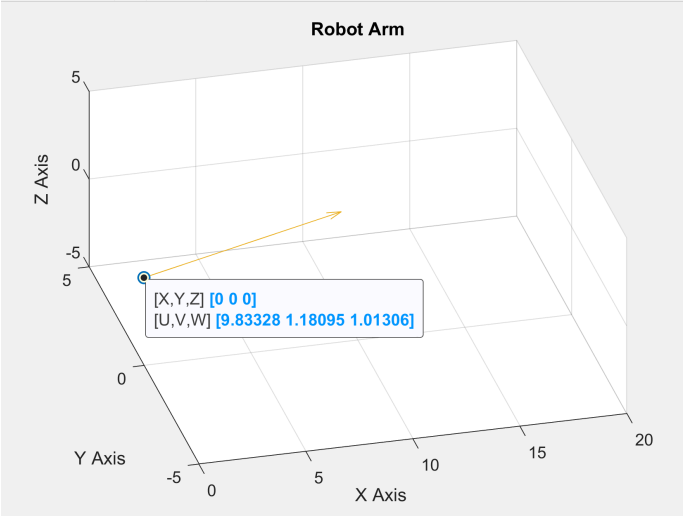

Figure 46: Catheter simulation

In addition to plotting the catheter in real time, MATLAB is also used to plot the trajectory the catheter tip takes when moving. This functionality is seen within the two dimensional plot function. In this function, a two dimensional plot of the xy, xz, and yz positions are plotted from the time the catheter started moving until the time the user terminates the system. A more in depth description of these results are described in 3. Results.

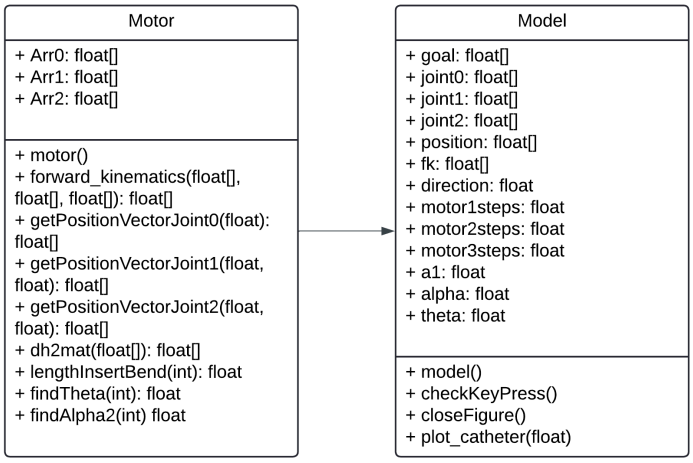

Figure 47: UML Class Diagram of Software

2.4 Final Design

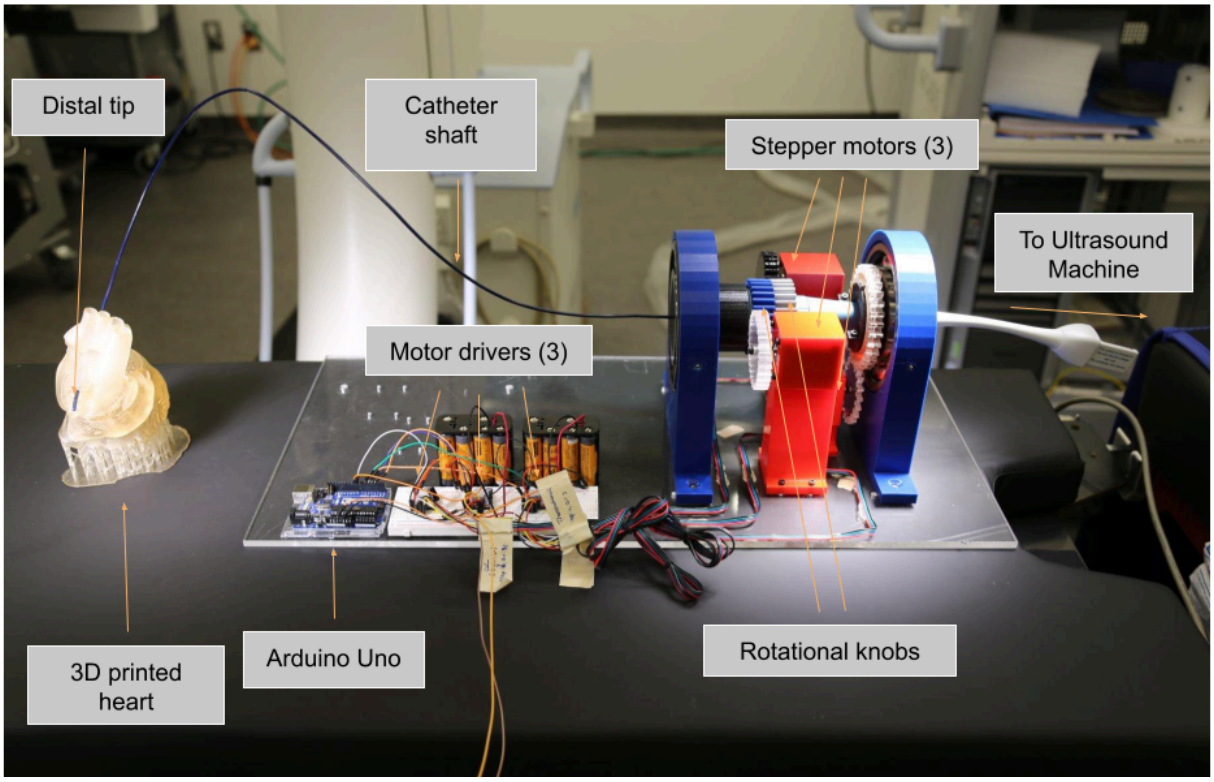

Figure 48: Assembled physical model of catheter seating device with ICE catheter in it.

The final mechanical design of the device is pictured in Figure 48 above. As described earlier in the report, all the components were modeled in Solidworks and then fabricated by 3D printing in PLA, and laser cutting on acrylic. The device is attached to an acrylic board to secure all of the components in place.

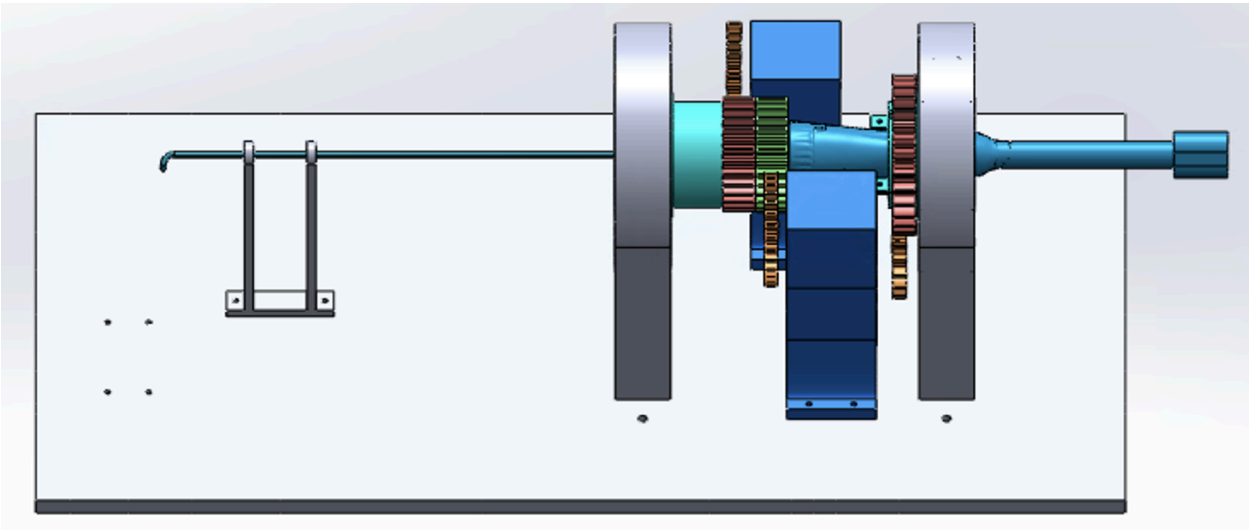

Figure 49: Assembled solidworks model of catheter steering device with ICE catheter model in it.

The robotic device replicates the movements of a clinician by providing three degrees of freedom to the catheter tip. The stepper motors power the orange gears that turn the knobs on the catheter to bend the tip in the XY and XZ planes. Finally, the last stepper motor turns the gear that rotates the entire catheter, providing the final degree of freedom. The catheter turns smoothly due to the ball bearings that support it on either end.

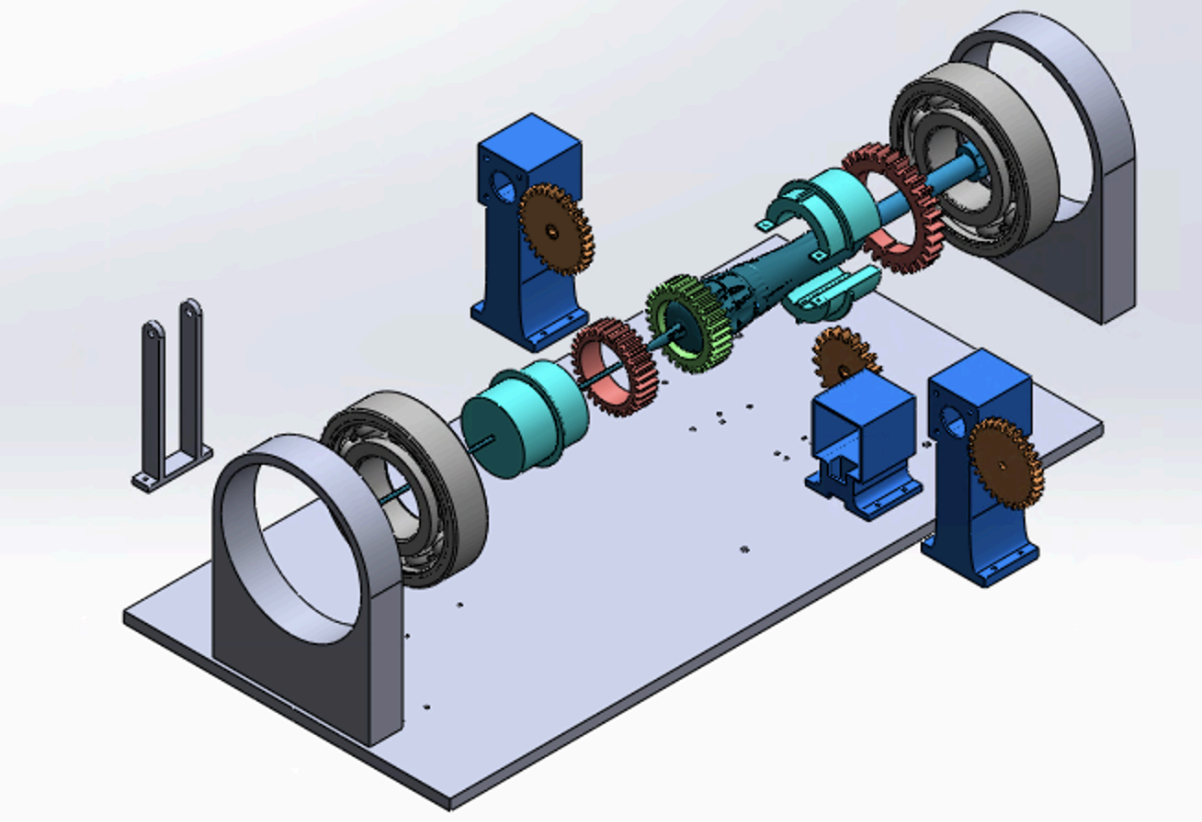

Figure 50: Expanded solidworks model of catheter steering device with ICE catheter model in it.

Overall the software implemented allowed the clinician to insert a keypress and move the catheter a certain amount of steps along with showing them a simulation of the catheter position. The software is implemented through the use of an Arduino and using the Matlab software. The motors are controlled through the Arduino software. When the clinician presses a key, the motor associated with that key turns a certain amount of steps. Simultaneously, a plot of the catheter's position is being simulated in Matlab. When a key gets pressed Matlab takes in the associated motor steps from Arduino. By converting these steps to degrees the forward kinematics of the system can be calculated. A model of the joint positions of the system was drawn to create a table of DH parameters. Using this table the degrees of movement can be plugged in to calculate a transformation matrix. From this, the new position of the catheter can be grabbed and plotted in the simulation. Each time a key is pressed the position of the catheter is updated in real time.

The hardware for this system consists of an Arduino Uno, three motor drivers, and three Nema-17 Stepper motors. The Arduino is the main control center of the system. As mentioned earlier, this microcontroller takes in the key inputs, converts them to steps and moves each motor. It does this by sending high and low signals to the motor drivers which then convert those to movements. Figure 51 shows the overall system architecture, highlighting the communication between the Arduino, MATLAB, and the stepper motors.

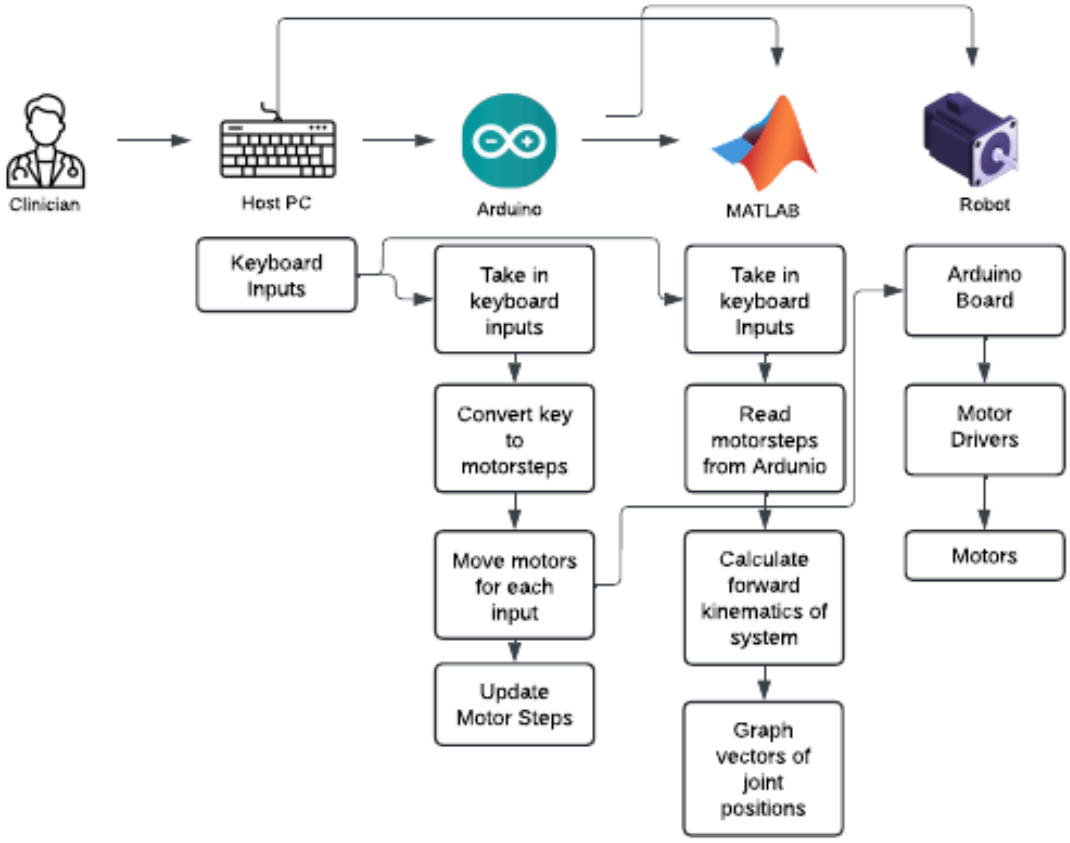

Figure 51: System Architecture

3. Results

By simulating the catheter tip in Matlab, its position can be compared to the real time position of the catheter. In order to validate the forward kinematics of the simulation, three tests were run for the trajectory of the catheter. These tests plotted the trajectory of the catheter as it moved. The graphs were compared to the motion of the catheter in real time. The graphs of the trajectories are shown below along with a picture of the catheter in the associated frame.

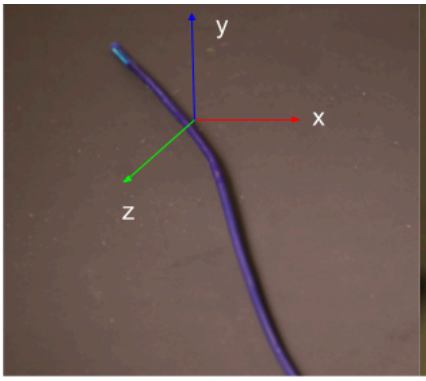

Figure 52a: Final position of catheter tip in X-Y plane

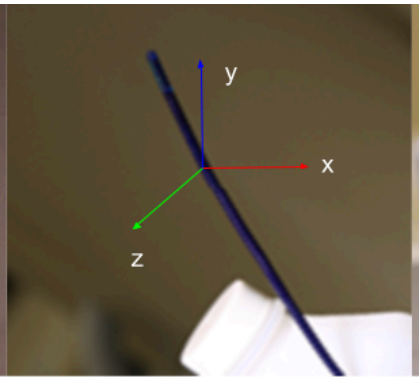

Figure 53a: Final position of catheter tip in Y-Z plane

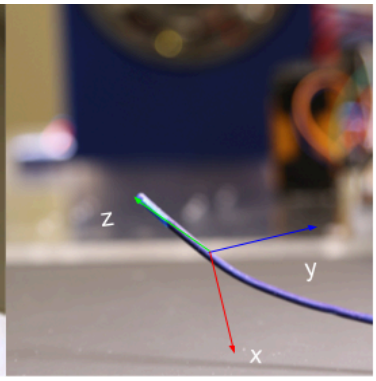

Figure 54a: Final position of catheter tip in X-Z plane

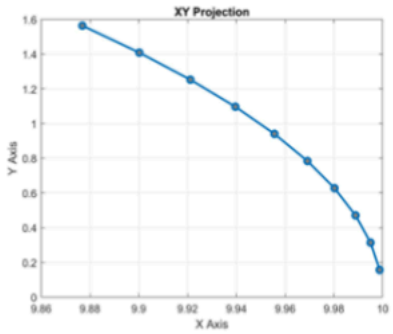

Figure 52b: Trajectory of catheter tip in X-Y plane

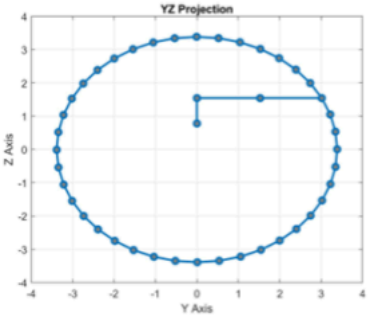

Figure 53b: Trajectory of catheter tip in Y-Z plane

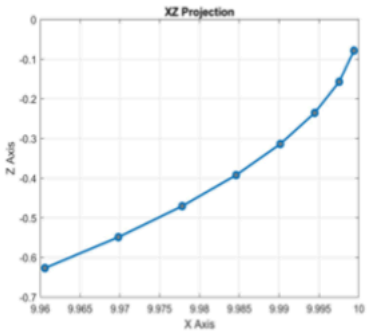

Figure 54b: Trajectory of catheter tip in X-Z plan

Figure 52b shows the trajectory of the catheter tip in the X-Y plane. In this simulation the catheter tip starts straight in the X direction. As the simulation progresses the catheter slowly bent more in the Y direction. This motion is clearly shown on the graph above. As the catheter moves it bends more in the Y direction and decreases its X coordinate.

Figure 53b shows the trajectory of the catheter tip in the Y-Z plane. In this simulation the catheter tip was bent and then turned 360 degrees. As shown, the catheter tip shows an accurate projection of this simulation. An oval shape can be seen in the graph.

Figure 54b shows the trajectory of the catheter in the X-Z plane. In this simulation the catheter starts straight in the x direction and bends in the Z direction. This motion is shown in the graph above. As the catheter bends in the negative Z direction the coordinate in the X direction slowly decreases.

By plotting the trajectories of the catheter in these three tests, the forward kinematics of the catheter tip was validated.

4. Discussion

The intracardiac catheter steering system builds the foundation for reducing clinician fatigue in cardiac catheterization procedures due to its teleoperation capabilities. Additionally, this system improves accuracy for position tracking through its simulation viewing, and if implemented across medical centers, it could reduce variability associated with the procedure. In designing and building this system, the team hopes that future teams can improve its functionality to match and improve upon existing experimental devices such as the ICE-steering system developed by the Harvard BioRobotics Lab.

Similarly to other devices that are being developed, such as the ICE-steering system developed by the Harvard BioRobotics Lab, the team's system allows for reduced clinician involvement in cardiac catheterization procedures [27]. Although the Harvard system accomplished its goals of autonomously steering the catheter, it involves complex gear trains involving gear belts, and buckling tubes and introducers on the catheter shaft [25]. Additionally, it is mounted on a scissor lift, creating a semi-bulky device to carry around [25]. The goal of this project was to create a simpler and more reproducible device that can be transported more easily than other devices on the market. This was achieved by developing a simple two-gear system to rotate each of the knobs and mounting the device between two ball bearings. Additionally, all the pieces are modeled in Solidworks and easily reproducible in different materials as the project progresses.

Future work for this project should begin with finding materials that can be sterilized in a clinical setting. As this was the first iteration of this project, the team did not focus on the materials being used, rather on streamlining the preliminary design. The second piece that should be addressed in the future is developing a linear translation component. The team faced several setbacks that prevented them from creating a high quality linear translation component, although some designs have been proposed. Future project groups can use these designs as a starting point for developing a linear translation component to provide 4 degrees of freedom to the system. The next step that future teams should look into is making the system completely autonomous. Again, due to project setbacks, the team determined that a more realistic goal was to make the system teleoperated. Lastly, in the distant future, other project groups could look into the imaging component of the system. This includes image processing techniques for two-dimensional ultrasound and the potential to implement artificial neural networks to accurately diagnose different heart conditions as the catheter traverses through the heart.

5. Broader Impact

This device is designed for the benefit of patients and clinicians alike, to reduce clinician fatigue and therefore the mistakes made during complicated intracardiac catheter procedures. However, the ethical considerations of this project must be discussed.

5.1 Societal and Global Impacts

An important consideration when designing a medical device is the potential to implement it on a global scale. There are many countries and locations that have less accessible medical care, and that would not have the wealth to afford an expensive robotic medical device. This device was designed to use less materials and be easily reproducible, resulting in a lower cost. Future improvements of the device will hopefully result in autonomous movement of the catheter, reducing the clinician experience required. This, and the ability to potentially remove the catheter to be able to manually control it creates a device that can be easily implemented across the country and the globe. The device is portable compared to other products on the market, being attached to a small acrylic board, as opposed to a large machine with a track on a hospital bed. It does require an external ultrasound to navigate still, used in conjunction with the ultrasound on the catheter tip, but should be able to be implemented anywhere that that catheter was used prior.

5.2 Environmental Impacts

Reducing the damage to the device allows it to be reused for a longer period of time and decrease the need to replace materials. Resources are limited by the environment, and developing a durable device creates a more environmentally sustainable product. This was accomplished in this device by choosing materials such as acrylic which would not deteriorate as fast as the PLA. Additionally, the method of manufacturing for the motor gears was changed to laser cutting from 3D printing, reducing the friction between the motor gears, knob gears, and rotation gear. This will increase the longevity of the gears. This iteration still includes a large amount of PLA which can not be reused, but in future implementations, the materials used will likely be changed.

5.3 Economical Impacts

On the economical side, this device was developed to alleviate the workload and fatigue of clinicians. The reduced time involvement of clinicians could affect the job market, however it should be a relatively insignificant change, as they still perform the majority of the procedure. This downside is outweighed by the potential benefits to patients from the clinicians' ability to focus in procedures without the tedious process of navigation of the catheter to the heart. Unfortunately, this device is built solely for the use of the AcuNav ICE catheter, and other

models can not be inserted into the system. This decreases the market for the device, since there is no potential for implementation with other types of catheters that are in use in hospitals.

5.4 Standards and Regulations

Because this device is a medical device, in the US it must go through U.S. Food and Drug Administration (FDA) regulations to ensure the safety and efficacy of the device. These codes are in place in order to prevent significant adverse events from occurring. A catheter is an invasive, temporary device, therefore it is classified as a Class II, or medium risk, medical device [29]. This classification requires submission of the FDA's 510(k), demonstrating that the device is substantially equivalent to other devices on the market and that there is a detailed risk management system [29]. Additionally, device tests to analyze durability, biocompatibility, mechanical properties and sterilizability are required prior to testing on human subjects [29]. These human trials are run on patients with their voluntary informed consent, with a plan approved by an institutional review board (IRB) [29]. These standards ensure that there is minimal harm to patients during testing and development of the device, complying with ethical principles.

6. References

[1] A. Ali *et al.*, “Catheter steering in Interventional Cardiology: Mechanical Analysis and Novel Solution,” *Proceedings of the Institution of Mechanical Engineers, Part H: Journal of Engineering in Medicine*, vol. 233, no. 12, pp. 1207–1218, Oct. 2019. doi:10.1177/0954411919877709 (1)

[2] A. Shrestha and A. Mahmood, “Review of Deep Learning Algorithms and architectures,” *IEEE Access*, vol. 7, pp. 53040–53065, Apr. 2019. doi:10.1109/access.2019.2912200 (2)

[3] B. Mahesh, “Machine Learning Algorithms - A Review,” *International Journal of Science and Research*, vol. 9, no. 1. doi:https://doi.org/10.21275/ART20203995 (2)

[4] “Cardiomyopathy,” Mayo Clinic, https://www.mayoclinic.org/diseases-conditions/cardiomyopathy/symptoms-causes/syc-20370709 (accessed Apr. 18, 2024).

[5] C. C. medical professional, “Heart surgery: Can it save or extend your life?,” Cleveland Clinic, https://my.clevelandclinic.org/health/treatments/17525-heart-surgery (accessed Apr. 21, 2024). (3)

[6] C. C. medical professional, “Minimally invasive heart surgery,” Cleveland Clinic, https://my.clevelandclinic.org/health/treatments/17233-minimally-invasive-heart-surgery#:~:text=How%20long%20does%20minimally%20invasive,about%20two%20to%20six%20hours (accessed Apr. 21, 2024). (4)

[7] C. J. Davidson and R. O. Bonow, “Cardiac Catheterization,” in Braunwalds Heart Disease, Philadelphia: Elsevier Saunders, 2008, pp. 383–405

[8] D. S. Dawoud and P. Dawoud, *Serial communication protocols and standards*, Sep. 2022. doi:10.1201/9781003339496 (5)

[9] D. Wu *et al.*, “Deep-learning-based compliant motion control of a pneumatically-driven robotic catheter,” *IEEE Robotics and Automation Letters*, vol. 7, no. 4, pp. 8853–8860, Oct. 2022. doi:10.1109/lra.2022.3186497 (6)

[10] G. Fagogenis et al., "Autonomous Robotic Intracardiac Catheter Navigation Using Haptic Vision," *Science Robotics*, Apr. 2019. [Online]. Available: https://www.science.org/doi/10.1126/scirobotics.aaw1977 (7)

[11] G. Perk et al., "Use of Real Time Three-Dimensional Transesophageal Echocardiography in Intracardiac Catheter Based Interventions," *Journal of the American Society of*

Echocardiography, vol. 22, no. 8, pp. 865-882, Jul. 2009. [Online]. Available: https://www.sciencedirect.com/science/article/abs/pii/S0894731709003939 (8)

[12] “Heart Valve Diseases: Types,” National Heart Lung and Blood Institute, https://www.nhlbi.nih.gov/health/heart-valve-diseases/types#:~:text=The%20three%20types%20of%20heart,%2C%20pulmonary%2C%20and%20tricuspid%20valves (accessed Apr. 18, 2024).

[13] I. Virgala et al., "Control of Stepper Motor by Microcontroller," *Journal of Automation and Control*, vol. 3, no. 3, pp. 131-134, 2015. (9)

[14] J. Goodenough and B. McGuire, *Biology of Humans: Concepts, Applications, and Issues*, Pearson, 2017. (10)

[15] John Hopkins Medicine, "Atrial Fibrillation Ablation," May 17, 2022. [Online]. Available: https://www.hopkinsmedicine.org/health/treatment-tests-and-therapies/atrial-fibrillation-ablation#:~:text=Ablation%20is%20a%20procedure%20to,signals%20that%20cause%20irregular%20heartbeats. (11)

[16] John Hopkins Medicine, "Fluoroscopy Procedure," Aug. 14, 2019. [Online]. Available: https://www.hopkinsmedicine.org/health/treatment-tests-and-therapies/fluoroscopy-procedure#:~:text=For%20intravenous%20catheter%20insertion%2C%20fluoroscopy,into%20joints%20or%20the%20spine. (12)

[17] John Hopkins Medicine, "Transesophageal Echocardiogram," Aug. 8, 2021. [Online]. Available: https://www.hopkinsmedicine.org/health/treatment-tests-and-therapies/transesophageal-echocardiogram. (13)

[18] John Hopkins Medicine, "Ventricular Tachycardia," Feb. 22, 2021. [Online]. Available: https://www.hopkinsmedicine.org/health/conditions-and-diseases/ventricular-tachycardia#:~:text=What%20is%20ventricular%20tachycardia%3F,t%20receive%20enough%20oxygenated%20blood. (14)

[19] J. Ryu et al., "Effect of Overhang and Stiffness on Accessibility of Catheter Tip to Lung Defects Under Surgical Constraints," *Annals of Translational Medicine*, vol. 8, no. 5, Mar. 2020. [Online]. Available: https://atm.amegroups.org/article/view/37246/html (15)

[20] M. Mhanna et al., "Steerable versus Nonsteerable Sheath Technology in Atrial Fibrillation Ablation: A Systematic Review and Meta-analysis," *Journal of Arrhythmia*, vol. 38, no. 4, pp. 570–579, Jun. 2022. [Online]. Available: https://doi.org/10.1002/joa3.12742 (16)

[21] M. Yin et al., "Mechanism and Position Tracking Control of a Robotic Manipulator Actuated by the Tendon-Sheath," *Journal of Intelligent & Robotic Systems*, vol. 100, pp. 849–862, Aug. 2020. [Online]. Available: https://doi.org/10.1007/s10846-020-01245-6 (17)

[22] Otvinta, "Bevel Gear Calculator," [Online]. Available: http://www.otvinta.com/bevel.html (18)

[23] P. L. N. Kapardhi, “Left Ventricular Dysfunction (LV Dysfunction): Symptoms, Causes, Diagnosis and Treatment,” CARE Hospitals, https://www.carehospitals.com/blog-detail/left-ventricular-dysfunction/ (accessed Apr. 18, 2024).

[24] P. M. Loschak et al., "Automatically Steering Cardiac Catheters in Vivo with Respiratory Motion Compensation," *The International Journal of Robotics Research*, vol. 39, no. 5, pp. 586–597, Feb. 2020. Available: https://doi.org/10.1177/0278364920903785 (19)

[25] P. M. Loschak et al., Robotic Control of Ultrasound Catheters for Intra-cardiac Visualization, https://biorobotics.harvard.edu/pubs/2016/contrib/PLoschak_Hamlyn_2016.pdf (accessed Apr. 21, 2024).

[26] R. A. Lange and L. D. Hillis, “Diagnostic Cardiac Catheterization,” AHA Journals, https://www.ahajournals.org/doi/10.1161/01.CIR.0000070982.94049.A2 (accessed Apr. 22, 2024).

[27] R. D. Howe, Harvard Biorobotics Lab, https://biorobotics.harvard.edu/ICEbot_.html (accessed Apr. 21, 2024).

[28] S. Kucuk and Z. Bingul, "Robot Kinematics: Forward and Inverse Kinematics," in *Industrial Robotics: Theory, Modelling and Control*, S. Cubero, Ed., pp. 117-148, Dec. 2006. [Online]. Available: http://www.intechopen.com/books/industrial_robotics_theory_modelling_and_control/robot_kinematics__forward_and_inverse_kinematics (20)

[29] U.S. Food & Drug Administration, "Overview of Device Regulation," [Online]. Available: www.fda.gov/medical-devices/device-advice-comprehensive-regulatory-assistance/overview-device-regulation#ide (21)

[30] V. Y. Reddy, "Mapping and Imaging," in *Cardiac Electrophysiology: From Cell to Bedside*, 6th ed., D. P. Zipes and J. Jalife, Eds., W.B. Saunders, 2014, pp. 581-593. Available: https://doi.org/10.1016/B978-1-4557-2856-5.00060-1 (22)

[31] “What are Congenital Heart Defects?,” Centers for Disease Control and Prevention, https://www.cdc.gov/ncbddd/heartdefects/facts.html (accessed Apr. 18, 2024).

[32] W. Yu, "PID Control in Task Space," in *PID Control with Intelligent Compensation for Exoskeleton Robots*, W. Yu, Ed., Mexico City, Mexico: Academic Press, 2018, pp. 35-53. Available: https://doi.org/10.1016/B978-0-12-813380-4.00003-7 (23)

[33] Y. Ganji and F. Janabi-Sharifi, "Catheter Kinematics for Intracardiac Navigation," *IEEE Transactions on Biomedical Engineering*, vol. 56, no. 3, Mar. 2009. [Online]. Available: https://ieeexplore.ieee.org/document/4760274 (24)

[34] Y. R. Manda and K. M. Baradhi, "Cardiac Catheterization Risks and Complications," StatPearls Publishing, Treasure Island, FL, Jun. 5, 2023. [Online]. Available: https://www.ncbi.nlm.nih.gov/books/NBK531461/